12-2007

Universal Voltage Rate Sensor Interface

Jayanth Chakradhar Kruttiventi
University of Tennessee - Knoxville

To the Graduate Council:

I am submitting herewith a thesis written by Jayanth Chakradhar Kruttiventi entitled "Universal Voltage Rate Sensor Interface." I have examined the final electronic copy of this thesis for form and content and recommend that it be accepted in partial fulfillment of the requirements for the degree of Master of Science, with a major in Electrical Engineering.

Jie Wu, Major Professor

We have read this thesis and recommend its acceptance:

Jay Frankel, Don W. Bouldin

Accepted for the Council:
Carolyn R. Hodges

Vice Provost and Dean of the Graduate School

(Original signatures are on file with official student records.)

To the Graduate Council:

I am submitting herewith a thesis written by Jayanth Chakradhar Kruttiventi entitled "Universal Voltage Rate Sensor Interface." I have examined the final electronic copy of this thesis for form and content and recommend that it be accepted in partial fulfillment of the requirements for the degree of Master of Science, with a major in Electrical Engineering.

_____
Jie Wu, Major Professor

We have read this thesis
and recommend its acceptance:

_____
Jay Frankel

_____
Don W Bouldin

Accepted for the Council:

Carolyn R. Hodges

_____

Vice Provost and Dean of the Graduate School

(Original signatures are on file with official student records.)

UNIVERSAL VOLTAGE RATE SENSOR

INTERFACE

Thesis Presented for the
Master of Science Degree
The University of Tennessee, Knoxville

Jayanth Chakradhar Kruttiventi
December 2007

ACKNOWLEDGEMENTS

I would like to express my sincere gratitude to my thesis advisor Dr. Jie Wu whose constant guidance, support and patience helped me in completing this thesis. I would also like to thank my thesis committee members Dr. Jay Frankel and Dr. Don W. Bouldin for their helpful suggestions and support in this work. I would like to mention specially thank to Dr. Frankel for his guidance and support during the course of documentation. I would like to thank National Science Foundation (contract number (CTS-06011236)) for funding my project titled “Universal voltage rate sensor interface”.

I thank my parents Mr. Hanumantha Rao, Smt. Rama sundari for their unconditional love and faith in me. They will always be my idols for life. The soul reason for me to be successful today is due to the encouragement and guidance they bared in me.

I would like to thank my sister Smt. Mamatha for her love and support. Her faith in me even in difficult circumstances always motivated me to achieve high goals. I would like to mention about my nephew Pardhavesa whose thought always brought a smile on my face. I would also like to thank my brother in law Mr. Mahidher.

I would to mention special thanks to my friends Archana, Naresh, Shashank, Bharadwaj and Lakshmi in UT for their constant encouragement. I will always remember Archana as a warm, caring person who used to get tensed for minor issues in day to day life. The support she provided is commendable. She will be a close friend forever. I have longing for the determination and effort Naresh puts, in every work in does. He is the one who will never back off from helping a friend in need. In Shashank, I can only say that I found a friend for life. We will always be friends who like to pull each others leg and

enjoy every moment of it. I will remember Bharadwaj, getting offended by the ways I portrayed as a savoir trying to correct his mistakes in life. He will be the person, who will be remembered by the entire group for the rest of our lifes. I recall Lakshmi as a small, short tempered girl who always starts a sentence with “eendi bey”. The trips we made as a group are memorable and I hope the group will remember me as a joyful person who always liked to pick on others mistakes.

I would also like to thank my engineering classmates Vitan, Raghu, Vikram, Rajshekar and Kiran. I recollect the days when we used to go to college on my bike and Vitan trying to explain me all the important points for days quiz. “All India Radio” was what I called Raghu, and he is and will always be a mysterious person who never used to reveal his future plans to others. The final year project I did with Vikram, “the wannabe dare devil” and Kiran “the wannabe Sharukhan” was a memorable experience. I hope Raj, the “moody one” trying to be obedient before his father will remember me after becoming a CEO. Our batch reminds me of the movie Dil chata hai where they go to Goa for a fun trip and only meet again in the climax of the movie.

Lastly, I would like to thank my old friends Kalyan, the guy whom I initially labeled as arrogant would be such a close friend for life. I always proudly tell people that there is an other guy in the world who is lazier than I. I would like to thank Amith “the video game guy” for being such a close friend in a short period of time.

I would lastly like to thank each and every one for being supportive and helpful.

ABSTRACT

Measurement of heat flux is required in many aerospace and heat treatment applications. Temperature data collected at embedded sites are noisy especially when measurements are taken in hostile environments. The predicted heat flux, when based on the rate of change of temperature, is more accurate than using temperature data as the latter data form is ill-posed. In the context of heat flux prediction, calculating the rate of change of temperature involves differentiation, which is the primary source of ill-posed effects.

This work involves developing a universal voltage rate sensor interface that minimizes these effects and also improves the signal-to-noise ratio. This is based on the concept of amplitude modulating the temperature data and differentiating it at a higher frequency. The proposed concept of improvement in signal-to-noise ratio was verified by the Matlab and PSpice simulations. The experimental outputs matched the simulations results.

TABLE OF CONTENT

TABLE OF TABLES

TABLE OF FIGURES

CHAPTER 1: INTRODUCTION

Sensors are a type of transducer which converts any physical properties into electrical signals. Sensors have become a highly active research area because of their potential of providing diverse services to broad range of applications, not only on science and engineering, but equally importantly on issues related to critical aerospace, defense and security, nuclear, health care, the environment, and the potential impact on the quality of all areas of life.

One of the major applications of the sensors is in temperature and flux analysis systems. A temperature sensor is a part of a temperature control system that detects the temperature and feeds this information to the control device. A perfect temperature sensor can be described as one which gives accurate reading and has no effect on the medium it is measured and the environment in which the reading is taken.

The major concern when measuring temperatures is to ensure that the measuring device is not affected by the surrounding environment. Accuracy of measurement using conventional sensor is inhibited as these sensors are used in various conditions, applications and thermal ranges.

Signal conditioning of sensor output becomes a major concern in these situations. Conditioning can be done in diagnostic and evaluation applications where the collected data can be analyzed at a later time. However, in applications like health monitoring system, arc jet heat flux measurement and reentry of satellites, there is less time for post processing.

Embedded sensors are used when the measurement with a probe is not possible in

the areas of interest. Figure 1.1 shows an example of arc-jet experiments, where thermocouple is mounted on the surface of a plate exposed to a high incoming heat flux which is used in hypersonic and reentry studies. Noise is one of the major concerns when measuring heat flux using embedded sensors. Using these noisy temperature data to estimate heat flux leads to an inverse problem where small changes in the input cause a large change in the output. This is not similar to normal applications where small changes in the input will leads to correspondingly smaller changes in the output. These effects are called ill posed as error amplification dominates.

The arc-jet heat transfer is known to be mathematically ill-posed[1,2,3,4] when temperature data are specified. In half-space heat conduction problems, the conventional linear heat equation in temperature is given by [1]

$$\rho C \frac{\partial T}{\partial t}(x,t) = k \frac{\partial^2 T}{\partial x^2}(x,t), \quad (x,t) \geq 0, \qquad [1.1]$$

where ρ is the density, C is the heat capacity and k is the thermal conductivity of the medium.

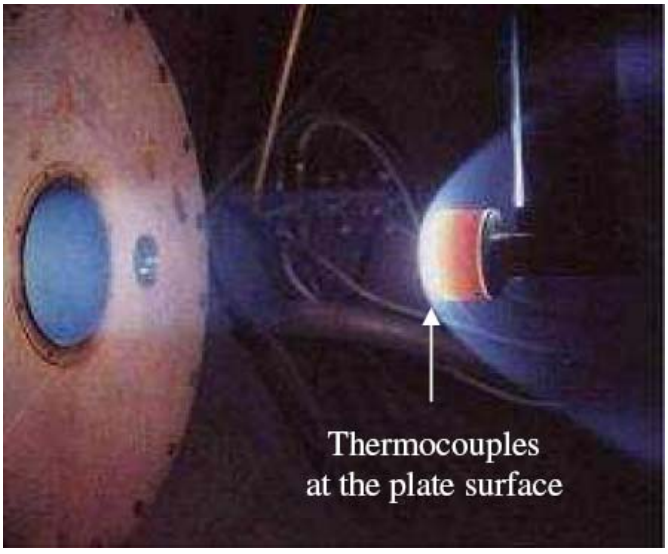

Figure 1-1:Embedded Transducer in Arc-jet experiment (Courtesy of NASA)

`

The heat flux is given by Fourier's law

$$q''(x,t) = -k\frac{\partial T}{\partial x}(x,t), \qquad [1.2\text{ a}]$$

where the basic energy balance is

$$-\rho c\frac{\partial T}{\partial t} = -\frac{\partial q}{\partial x} \qquad [1.2\text{ b}]$$

Using these equations, we can express the heat equation in terms of heat flux, q''(x,t)

$$\frac{1}{\alpha}\frac{\partial q''}{\partial t}(x,t) = \frac{\partial^2 q''}{\partial x^2}(x,t), \quad (x,t) \geq 0, \qquad [1.3]$$

where α is thermal diffusivity and is given by α = k/(ρC). The relationship between heat flux and temperature within the half space can be given by using classic integral solution

$$T(x,t) = \sqrt{\frac{1}{\rho Ck\pi}}\int_{u=0}^{t} q''(0,u)\frac{e^{-\frac{x^2}{4\alpha(t-u)}}}{\sqrt{t-u}}du, \quad (x,t) \geq 0, \qquad [1.4]$$

which when evaluated at the boundary conditions at x=0, yields

$$T(0,t) = \sqrt{\frac{1}{\rho Ck\pi}}\int_{u=0}^{t} \frac{q''(0,u)}{\sqrt{(t-u)}}du, \quad t \geq 0. \qquad [1.5]$$

Using this equation, we can calculate the surface temperature if we are provided with the heat flux data. As the solution involves integration, it is numerically stable, even if there is noise present in the flux data with no bias present. Heat flux is calculated from temperature data using the Abel integral equation obtained by inverting Eq[1.5] to get

$$q''(0,t) = \sqrt{\frac{\rho Ck}{\pi}}\int_{u=0}^{t} \frac{\partial T}{\partial u}(0,u)\frac{du}{\sqrt{(t-u)}}, \quad t \geq 0. \qquad [1.6]$$

Finding the heat flux using discrete noisy surface temperature data is unreliable as the process is ill-posed. A system is called ill-posed if small changes in the input cause

large changes in the output. This calculation is unstable because it involves numerical differentiation which is known to be ill-posed.

The fundamental problem with electrical differentiators is that the gain of the signal is proportional to the signal frequency. The high frequency components in the input signal are amplified more than the low frequency components. If we are dealing with a signal of low frequency (100 Hz) as is the case with many heat transfer diffusion applications, gain of the signal is very low. But the noise which is uniform in all frequencies is amplified more at high frequencies. This will cause the signal-to-noise ratio to decrease at the output. It has been proven that if temperature data is contaminated with white noise in Eq[1.6], then the root-mean-square (RMS) surface heat flux error grows as $\sqrt{N}$ where N is the sample size [2].

Filtering is performed to eliminate these problems which are mainly caused by high frequency components. Low pass filtering is a simple way to eliminate the unwanted high frequency components and will also improves the signal to noise ratio. This is depicted in Figure 1.2. The signal to noise ratio of a corrupted signal is $|c|^2$ which has a noise power of $|N|^2$. After the signal is filtered the signal to noise ratio increased.

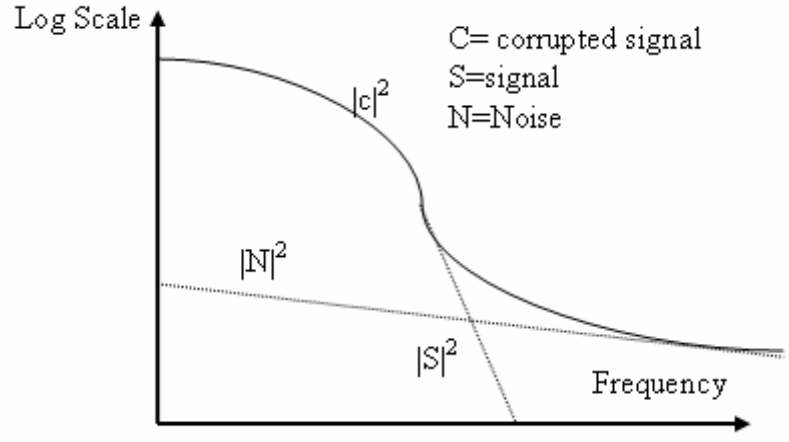

Figure 1-2:Signal to noise ratio in Frequency domain

`

Gauss low pass filter [1] is used to eliminate high frequency noise in the data because of the advantages it offers both in frequency and time domain. The Fourier transform of a Gauss function in time produces another Gauss function in frequency, thus eliminating 'wiggles' from both frequency and time domain. An inspection of the power spectral density of the input signal will indicate the cutoff frequency, ω_c. This low-pass filter offers good differentiability properties i.e., it does not have any side-lobes. The filter produces an analytic function i.e., it converted a finite number of samples in the original data to infinite so they can be analytical differentiated.

Heating/cooling rate can be obtained by differentiating the filtered temperature data. Heat flux predicted using this data can improve signal-to-noise ratio. The equation used for finding heat flux using rate information is given by [1]

$$q''(0,t) = \sqrt{\frac{\rho C k}{\pi}} \int_{u=0}^{t} \frac{\partial T}{\partial u}(x,u) \frac{du}{\sqrt{(t-u)}}, \quad (x,t) \geq 0. \qquad [1.7]$$

A discrete representation of the above equation is [1]

$$q''_{f,i} = \sqrt{\frac{\rho C k}{\pi}} \sum_{j=0}^{i=1} \frac{dT_{f,i}}{dt} (\sqrt{t_i - t_j} - \sqrt{t_i - t_{j+1}}), \quad i = 1,2,.....N, \qquad [1.8]$$

where $T_{f,i}$ is the filtered temperature data which is sampled uniformly, i.e. $t_j = j\Delta t$ where $\Delta t = t_{max}/N$.

Using the surface heating/cooling rate instead of surface temperature leads to stabilization of the heat flux. The RMS error of heat flux decreases as $\sqrt{\log(N)/N}$ as N increases [2]. For improving the signal to noise ratio one has to increase the sampling rate of temperature data.

`

Figure 1.3 compare the RMS heat flux error in calculated heat flux data using both temperature and heating rate data [3]. It compares results using two different white noise factors ε_1 and ε_2. Note the gradual increase in RMS error when temperature data are used to find the heat flux. The RMS heat flux error is reduced when the noise factor is low. In contrast the RMS heat flux error reduces gradually as the number of samples increase when heat flux is predicted using rate data. Therefore, using heating/cooling rate data allows for accurate real-time heat flux predictions that are critical to health management and diagnostics. Using an infinite sample signal i.e. analog signal instead of digital signal will reduce the RMS error even further.

Figure 1.4 shows simulated data of temperature and the predicted heat flux using Eq[1.8]. As the simulated input temperature data is coupled with noise the predicted heat flux data is unusable. But if the differentiated data is used, (Figure 1.4c), the predicted heat flux nearly reconstructs in to a Gauss shaped solution (Figure 1.4d). Thus a usable heat flux is available from differentiated data even if the noise is eight times higher than the temperature data. Details of the particular heat transfer study can be found in [4].

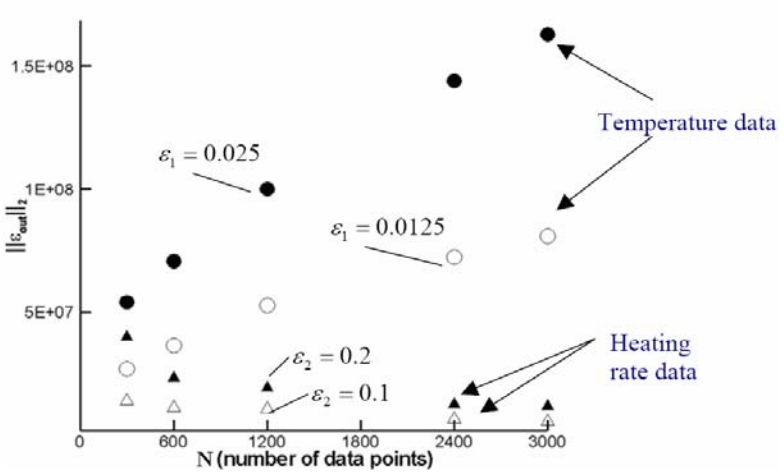

Figure 1-3: Root Mean Square error of the surface heat flux with sample size N (Taken from [3])

`

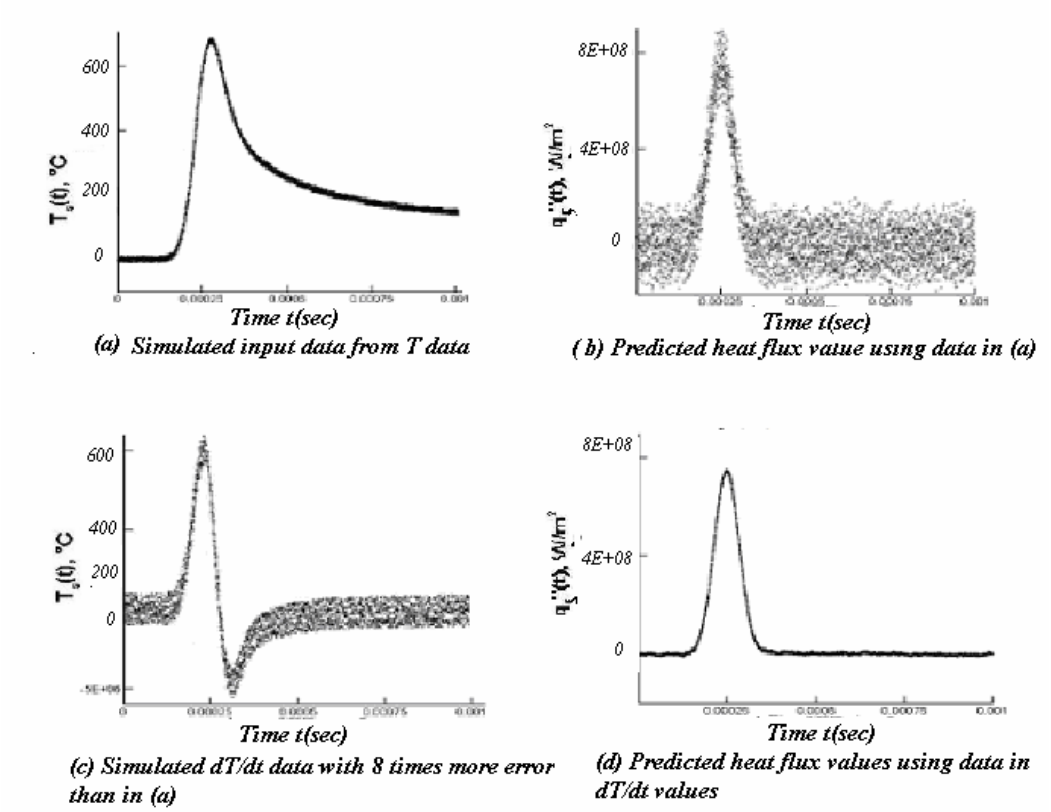

Figure 1-4: Heat flux using Temperature data and heating/Cooling rate (Taken from [4])

As previously discussed, two techniques have been proposed to estimate heat flux namely; filtering the temperature data and differentiating the temperature data using digital filtering. There are still some problems in these processes [5]. Firstly, filtering does not remove all the noise components present in the input signal and differentiation of this signal is still affected by noise. Secondly, differentiator gain depends on input frequency. The latter problems can be avoided if the input signal is of high frequency.

Consider the temperature signal shown in Figure 1.5 [4]. The resulting power spectral density shows that frequency components are below 100 Hz. During differentiation, different frequency components are amplified to different voltages. For example, if the

`

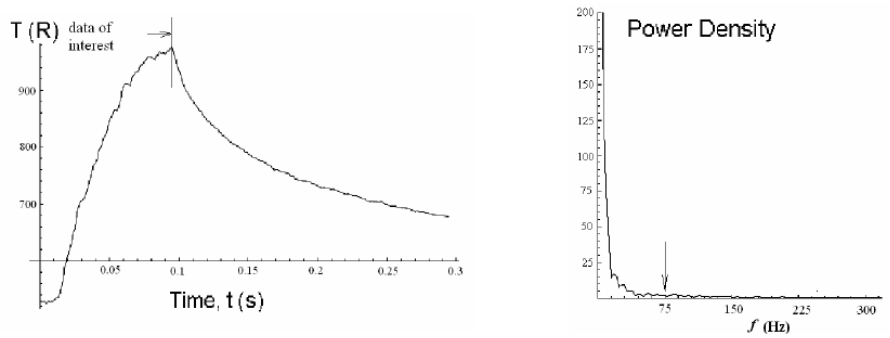

Figure 1-5: Temperature data and power spectral density[taken from [4]]

noise components that vary between 50 Hz to 150 Hz whose magnitude of one, the magnitude of the output voltage of the differentiator using a capacitor value of 10 μf and resistor of 1 KΩ, will vary between 3.14 V to 9.42 V.

The error caused by differentiation is minimized if we shift the temperature voltage data obtained from thermocouple to higher frequencies using amplitude modulation. If the AM signal is differentiated at this frequency, modulated differentiated temperature data can be extracted from it by removing all the unnecessary components. This signal can be demodulated to obtain the desired differentiated signal.

If the same low input signal is amplitude modulated with a carrier frequency of 1 MHz frequency, the signal is shifted around the carrier frequency. Lower side-lobe will vary between 999,850 Hz and 999,950 Hz. Using a differentiator with capacitor of 5 ηf and resistor of 1 KΩ, the gain will vary between only between 3.1411 V and 3.1414 V.

As we can see signal-to-noise ratio can be considerably increased by amplitude modulating the signal and differentiating the signal at the higher frequencies. If the signal has a pass band of 1 to 100Hz, the signal has a 100% change in frequency domain. But if the signal is amplitude modulated by a carrier of 1 MHz the variation will be less than 0.01% from 1 K to 1.0001 MHz. The noise will also be affected by the same ratio.

`

These principles are followed when developing a universal voltage rate sensor interface which inputs the temperature data from the sensor and produces the heating/cooling rate for finding heat flux. The general outline of the steps followed in developing this interface can be broken down into following steps

1) Obtaining the noisy, temperature data from the embedded site through an in-situ thermocouple
2) Finding the power spectrum of the signal and estimating the cutoff frequency for the filter
3) Filtering the noisy data
4) Amplitude modulating the signal with a carrier frequency much higher than the highest frequency in the pass band of the input signal
5) Differentiating the amplitude modulated signal
6) Extracting the differentiated modulated signal by removing the unnecessary components using signal manipulation
7) Demodulating the signal to obtain the heating/cooling rate
8) Finding the heat flux using the rate data and using Eq[1.8]

This rate information does not need any signal processing and can be directly used to find the heat flux information in real time. The block diagram of the proposed model is shown in Figure 1.6.

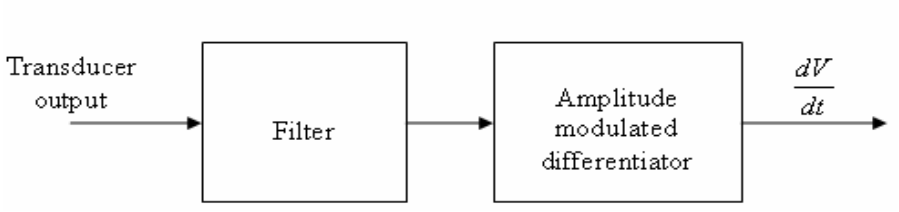

Figure 1-6: Block diagram of proposed model

`

Developing of universal voltage-rate interface involves developing a hardware interface between the actual in-situ sensor and the analysis software which improves the signal- to-noise ratio of the temperature sensor. This is an add-on to the existing hardware infrastructure so the cost of up gradation reduces. We can also obtain higher order derivatives if these blocks are placed in a cascade structure. This project concentrates on developing an amplitude modulated differentiator for diffusive heat flux studies.

The concept of amplitude modulation and the procedure followed to extract the differentiated component is discussed in the Chapter 2. Chapter 3 covers Matlab simulations first on a single-tone sinusoidal signal and later on a noisy temperature data. The improvement in the signal-to-noise ratio with increase in carrier frequency and also with different sampling rate is verified. Chapter 4 covers the design and simulation for hardware developed. Orcad PSpice is used to perform simulations for the op amp models. Finally, chapter 5 presents the experimental results and the SNR obtained and the problems encountered. Chapter 6 presents the conclusions and future work

CHAPTER 2: AMPLITUDE MODULATION DIFFERENTIATOR

The amplitude modulation differentiator forms the fundamental building block of universal voltage-rate sensor interface. The method of extracting a differentiated signal after amplitude modulation and differentiation is presently explained. The concept of general amplitude modulation and double sideband suppressed carrier modulation are discussed and the advantages of using DSBSC are explained. The method of extraction of the desired signal after amplitude modulated differentiation is also explained using a single-tone frequency signal.

2.1 Amplitude Modulation

Amplitude modulation is defined as a process in which the amplitude of the carrier wave $c(t) = A_c \cos(2\pi f_c t)$ is varied about a mean value, linearly with the baseband signal **m(t)** [6]. Here A_c is the magnitude and f_c is the frequency of the carrier wave. The amplitude modulated wave can be described as a function of time in the form

$$AM(t) = A_c[1 + k_a m(t)]\cos(2\pi f_c t) \qquad [2.1]$$

where k_a is the modulation index, If we assume the modulating signal to be a sine wave as shown in Figure 2.1(a) the modulated signal is shown in Figure 2.1(c). The carrier wave is also shown as Figure 2.1(b). We can observe that the envelope of the carrier wave follows the modulating signal in both positive and negative side of the y axis.

The amplitude of AM wave as shown in Eq[2.1] is [1 + k_am(t)]. Modulation factor (|k_am(t)|) determines the amount to which the carrier wave is being modulated by

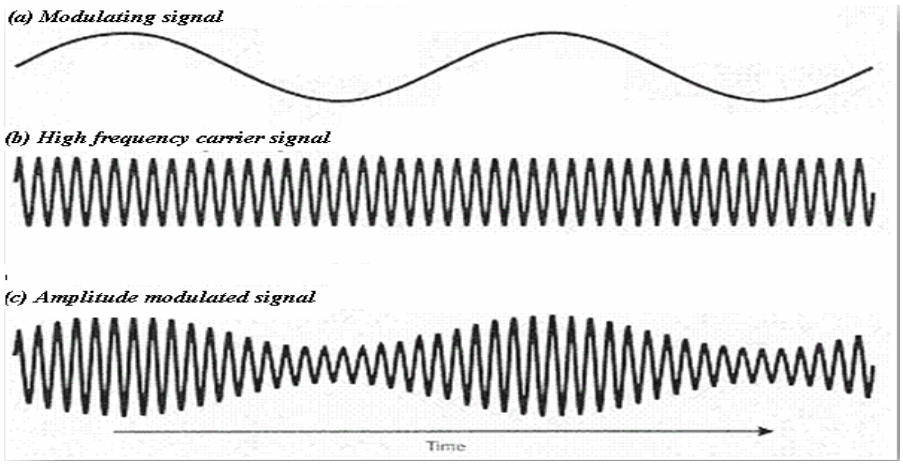

Figure 2-1: (a) Modulating signal (b) Carrier signal (c) Amplitude modulated signal

the modulating signal. If AM_{max} and AM_{min} are the maximum and minimum values of the envelope signal, the modulation factor, μ can be given by

$$\mu = \frac{A_{\max} - A_{\min}}{A_{\max} + A_{\min}} \qquad [2.2]$$

To avoid over modulation which results in a phase shift where ever the envelope crosses zero value, we must ensure that the μ is always be less than 1. But if μ is greater than unity, A_{max}-A_{min} is greater than A_{max}+A_{min} and envelope is phase shifted as both the envelopes crosses over. Demodulation of phase shifted signal using ordinary methods will not produce the desired results. If the modulation factor is multiplied by 100 then it is called the modulation index of the system.

The frequency spectrum of the AM signal can be found by applying the Fourier transform to Eq [2.1]

$$AM(f) = \frac{Ac}{2}\left[\delta(f - fc) + \delta(f + fc)\right] + \frac{kaAc}{2}\left[M(f - fc) + M(f + fc)\right] \qquad [2.3]$$

If a modulating signal m(t) is band-limited with the spectrum M(ω) as shown in Figure 2.2(a), then the corresponding frequency spectrum of the modulated signal is shown in

`

Figure 2.2(b)

The band of frequencies above the carrier frequency is called the upper sideband, and band below is called lower sideband. Here the carrier wave is completely independent of the modulating signal and it can be suppressed. If the carrier wave is suppressed from the AM wave it is called double side band suppressed carrier wave form or (DSBSC).

2.2 2.2 Double side band suppressed carrier

The DSBSC modulation consists of the product of the modulation signal m(t) and the carrier wave c(t)

$$AM_{DSBSC} = A_c m(t)\cos(2\pi f_c t) \qquad [2.4]$$

As the envelope of the modulated signal is dependent upon the amplitude of the modulating signal, AM_{DSBSC} wave undergoes a phase reversal every time it crosses zero. This phase reversal is seen in Figure 2.3(a). The frequency components measured using the Fourier transform of this AM signal

$$AM_{DSBSC}(f) = \frac{1}{2} A_c \left[M(f - fc) + M(f + fc) \right] \qquad [2.5]$$

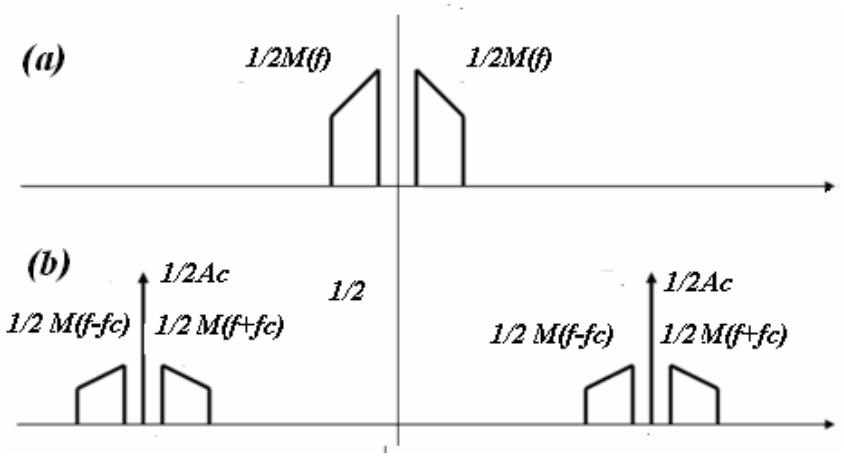

Figure 2-2:(a) Spectrum of the Modulating signal (b) Frequency spectrum of the AM signal

`

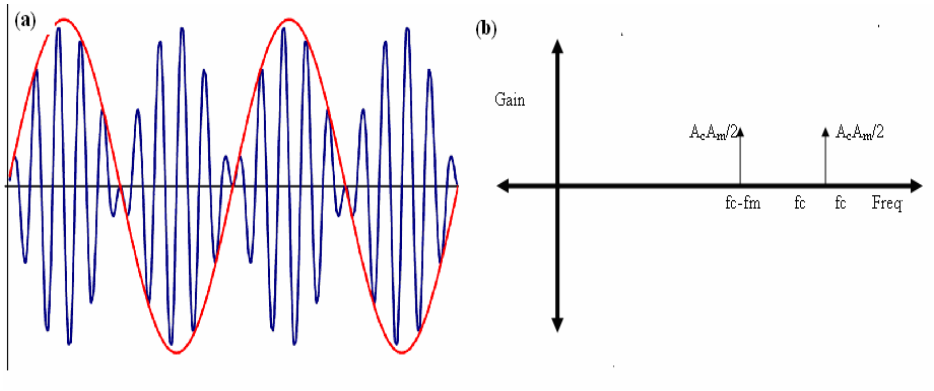

Figure 2-3: Double side band suppressed carrier Amplitude Modulation

Note that there are only two frequency components at the output and the carrier is suppressed Figure 2.3(b). In both simulated and real experiments, the modulation is done using DSBSC because of its mathematical simplicity and no extra terms to be dealt with during differentiation. But demodulation of DSBSC is different from that of AM wave and appropriate technique needs to be used.

2.3 Mathematical proof

Direct differentiation of amplitude modulated wave does not result in differentiated amplitude modulated wave. Manipulation of the wave is necessary before the differentiated signal can be extracted from it. If a modulating signal m(t) and carrier signal c(t) are amplitude modulated we get

$$AM(t) = c(t)m(t) \qquad [2.6\ (a)]$$

If this signal is differentiated we get

$$AM'(t) = c'(t)m(t) + m'(t)c(t) \qquad [2.6\ (b)]$$

The required component is the amplitude modulated signal of differentiated modulating and carrier wave. This is the second term in the Equation 2.6 which can be

extracted by selectively choosing this desired frequency components and filtering the unnecessary ones.

There are two important factors that have to be taken into consideration for doing this. First, the amplitude modulated signal is divided into two groups of frequencies, the lower and upper side bands. Second, during differentiation, different frequencies are amplified with different gain. The technique to remove the undesired components after differentiation should also take these factors into consideration.

The procedure of extracting the differentiated component is explained with the help of two single tone signals. This theory will also apply to pass band signals. If we consider a single tone modulating signal $m(t)=A_m\cos(w_m t)$ and the carrier wave to be at frequency f_c which can be expressed as $c(t) = A_c\cos(w_c t)$

$$AM(t) = A_m A_c \cos(\omega_c t)\cos(\omega_m t) \qquad [2.7]$$

This can be written as sum of two frequency components as

$$AM(t) = \frac{A_m A_c}{2}\left[\cos(\omega_c - \omega_m)t + \cos(\omega_c + \omega_m)t\right] \qquad [2.8]$$

The transfer function of the differentiator is shown in Eq[2.9]

$$Vout = -RC\frac{dV}{dt} \qquad [2.9]$$

Frequency response of the differentiator is shown in Figure 2.4. Here different frequency signal are amplified to different gains. As amplitude modulated signal has two different frequencies at $\omega_c-\omega_m$ and $\omega_c+\omega_m$, they will be amplified with different gains

$$\frac{dAM(t)}{dt} = -RC\frac{A_m A_c}{2}\left[-(\omega_c - \omega_m)\sin(\omega_c - \omega_m) - (\omega_c + \omega_m)\sin(\omega_c + \omega_m)\right] \qquad [2.10]$$

If we assume that the total gain of differentiator at frequency $\omega_c-\omega_m$ is A_1 and the gain at frequency $\omega_c+\omega_m$ is A_2 ($A_2 > A_1$). It can be simplified and written in the form of

`

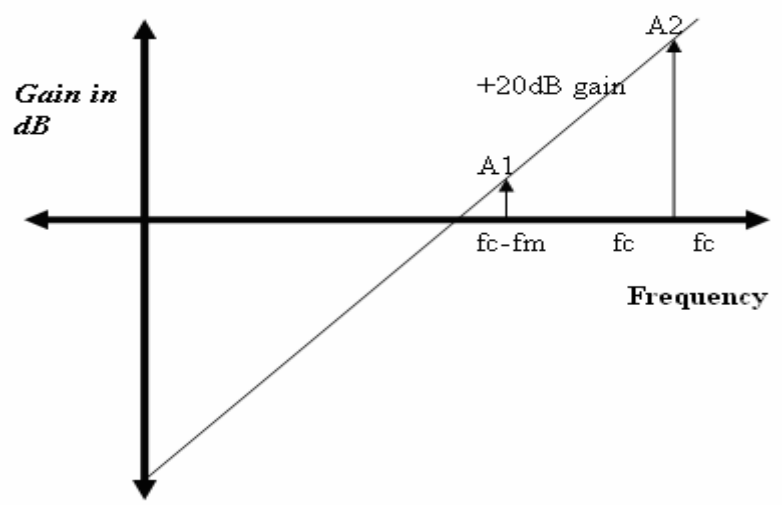

Figure 2-4: Frequency response of the differentiator

$$\frac{dAM(t)}{dt} = \left[A_1 \sin(\omega_c - \omega_m) + A_2 \sin(\omega_c + \omega_m)\right] \qquad [2.11]$$

Simplifying Eq[2.11] can be written as

$$\frac{dAM(t)}{dt} = \left[A_1\left(\sin(\omega_c t)\cos(\omega_m t) - \cos(\omega_c t)\sin(\omega_m t\right) + A_2\left(\sin(\omega_c t)\cos(\omega_m t) + \cos(\omega_c t)\sin(\omega_m t)\right)\right]$$

This can be further simplified into

$$\frac{dAM(t)}{dt} = \left[(A_1 + A_2)\left\langle\sin(\omega_c t)\cos(\omega_m t)\right\rangle + (A_1 - A_2)\left\langle\cos(\omega_c t)\sin(\omega_m t)\right\rangle\right] \qquad [2.12]$$

Where

$$A_1 + A_2 = RCA_m A_c \omega_c \qquad [2.13\ (a)]$$

$$A_1 - A_2 = RCA_m A_c \omega_m \qquad [2.13\ (b)]$$

The differentiation contains two components, the desired component, $\cos(\omega_c t)\sin(\omega_m t)$ and the undesired component, $\sin(\omega_c t)\cos(\omega_m t)$. If the undesired component is generated and subtracted from the input we are only left with the differentiated input amplitude modulated wave. This can be demodulated to obtain the desire result.

`

2.4 Disadvantages of using a phase shifter

The block diagram proposed to generate the undesired component as discussed in [4] is shown in Figure 2.5. Here the signal is first passed through a low pass filter to remove the unnecessary noise components. This is then amplitude modulated using a carrier generated from the oscillator. The differentiated signal of the amplitude modulated wave is summed with the phase shifted amplitude modulated wave. Here the phase shifted wave produces the undesired component. The output from the summer is demodulated to obtain the desired results.

If we phase shift the amplitude modulated wave given by Eq[2.8] through 90 deg we get

$$PS(AM(t)) = \frac{A_m A_c}{2}\left[-\sin(\omega_c - \omega_m)t - \sin(\omega_c + \omega_m)t\right] \qquad [2.14]$$

Eq[2.14] can be simplified to

$$PS(AM(t) = \frac{A_c A_m}{2}\left[-\left[\sin(\omega_c t)\cos(\omega_m t) + \cos(\omega_c t)\sin(\omega_m t)\right] - \left[\sin(\omega_c t)\cos(\omega_m t) - \cos(\omega_c t)\sin(\omega_m t)\right]\right]$$

which further simplifies to

$$PS(AM(t)) = -AcAm\left[\sin(\omega_c t)\cos(\omega_m t)\right] \qquad [2.15]$$

If this signal is amplified to a magnitude given by Eq[2.13 (a)] and passed to the summer along with the differentiated amplitude modulated signal given by Eq[2.12], we will get the desired result.

There are many difficulties while implementing this in hardware circuits. Generally a phase shifter is designed to produce the desired phase shift at a particular frequency. As AM signal is the sum of two frequencies, we can not phase shift these two frequencies to the same phase. To achieve this we have to design a complicated phase

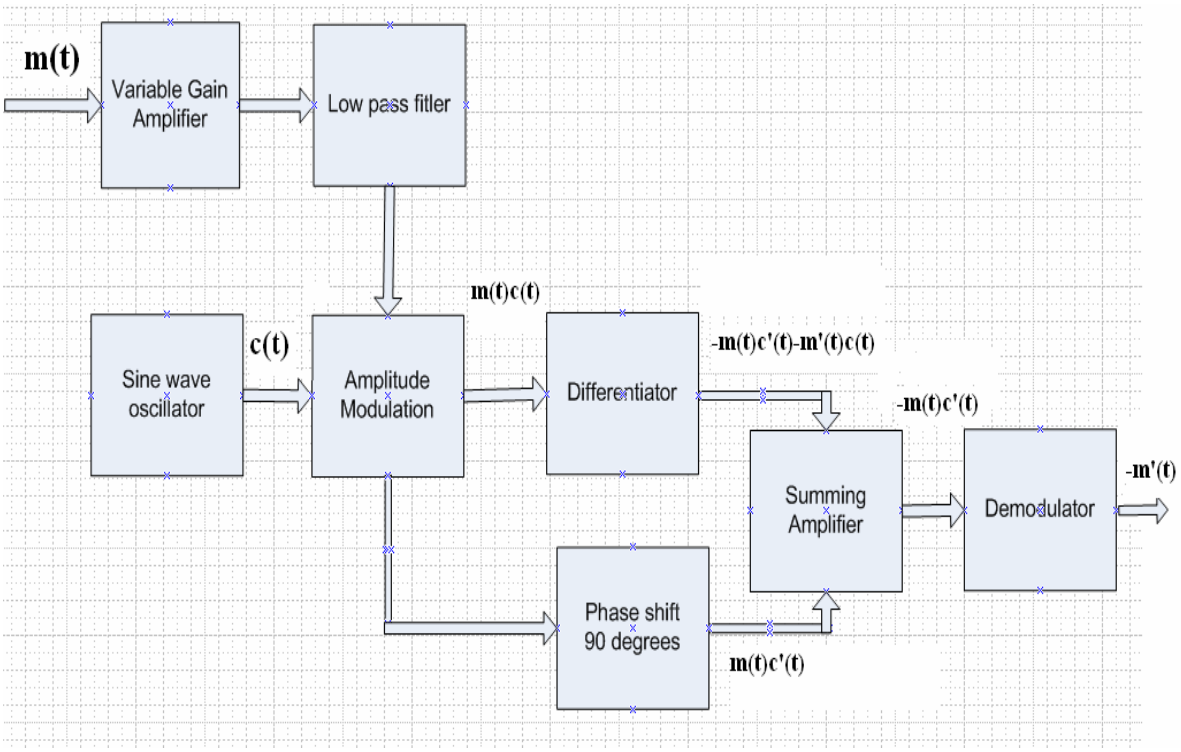

Figure 2-5: Amplitude modulation differentiation using a phase shifter

shifter which is independent of frequency.

Even if a phase shifter independent of frequency is designed, the amplitude of the undesired signal from the phase shifter will not match the signal at the output of differentiator. Additional variable gain amplifier is required whose gain has to be varied for different signal has to used after the phase shifter.

2.5 Changes to the current model

This problem can be avoided, if the modulating signal is amplitude modulated with the differentiated carrier wave. Differentiating the carrier wave amplifies the signal to the desired level and eliminates further amplification. The modified block diagram is shown in Figure 2.7. In the modified block diagram, we have two differentiators and two amplitude modulation blocks.

`

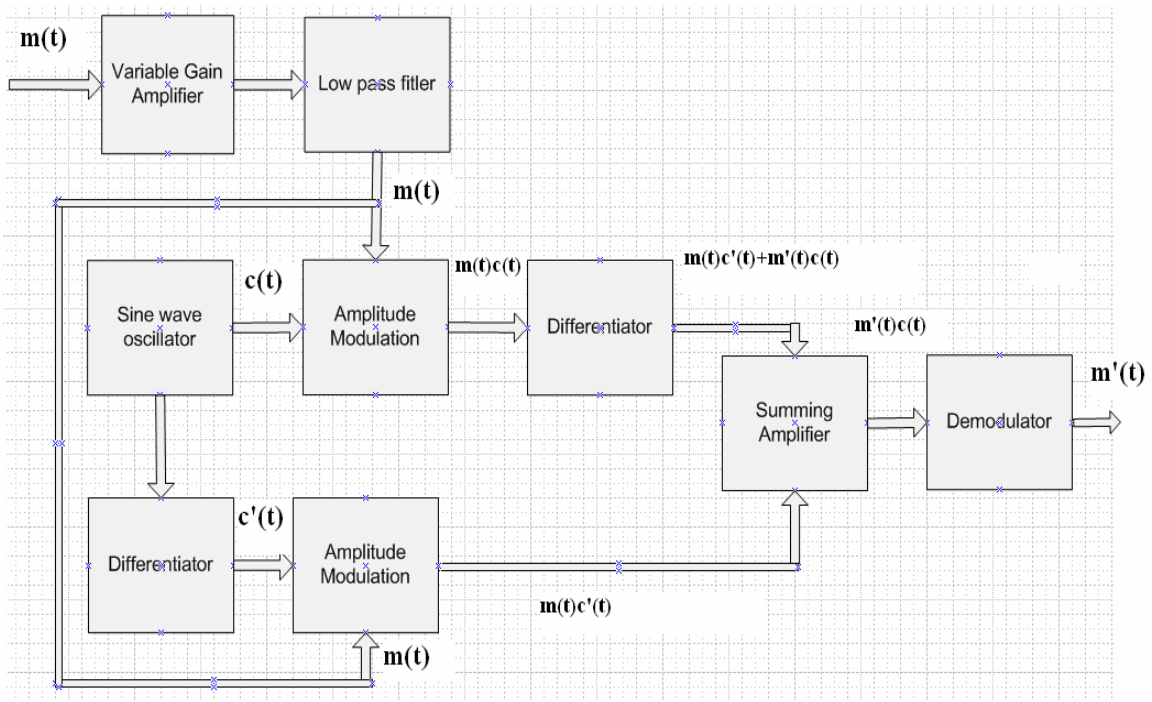

Figure 2-6: Modified block diagram with an extra differentiator and amplitude modulator

From the carrier signal, we give one branch to the amplitude modulation and another branch to the differentiator. The amplitude modulated signal is differentiated and given to the summing amplifier. The differentiated carrier is also amplitude modulated with the modulating signal and the given to the summing amplifier. The output of the summing amplifier should contain the amplitude modulated content of the differentiated modulated signal. This component is demodulated to obtain the desired differentiated input signal. We expect this signal to contain less noise than the signal differentiated at lower frequencies.

If the carrier is differentiated we get and amplitude modulated we obtain

$$dc(t) = -RCA_c\omega_c \sin(\omega_c t) \qquad [2.16]$$

If this signal is used as a carrier signal in amplitude modulation, we get

$$Am\_dc(t) = -RCA_m A_c \cos(\omega_m t)\sin(\omega_c t) \qquad [2.17]$$

`

The amplitude component of the obtained signal is equal to the Eq[2.13(a)], A_1+A_2, but with a negative sign. Adding this component to the differentiated AM signal results in an AM signal, which is a product of carrier and differentiated modulating signal. The output magnitude of the summer, after the undesired component is removed is a multiple of (A_1-A_2). This is only dependent on the modulating frequency and gain the of the differentiator and does not depend on the carrier frequency

2.6 Demodulation of DSBSC

The output from the summer should be demodulated to obtain the desired differentiated modulated signal. The method used for this purpose is depicted in the Figure 2.7. The carrier wave which is used to generate the AM signal is used for this purpose. This carrier signal must be product modulated with the output of the summer. The resultant signal should be passed through a low-pass filter to remove high frequency components.

The output from the summer is given by

$$S(t) = (A_1 - A_2)\sin(2\pi f_m t)\cos(2\pi f_c t) \qquad [2.18]$$

where A_1-A_2 is the magnitude of the output which is given by Eq [2.13(b)] and $\sin(2\pi f_m t)$ is the differentiated modulated signal.

If this output from the summing amplifier is multiplied with the carrier signal then we obtain

$$S1(t) = (A_1 - A_2)\sin(2\pi f_m t)\cos(2\pi f_c t) A_c \cos(2\pi f_c t)$$

$$\text{or} \quad S1(t) = \tfrac{1}{2} A_c (A_1 - A_2)\sin(2\pi f_m t)\cos(2\pi 2 f_c t) + \tfrac{1}{2} A_c (A_1 - A_2)\sin(2\pi f_m t) \qquad [2.19]$$

This equation has two terms; the first is the AM of differentiated modulating

`

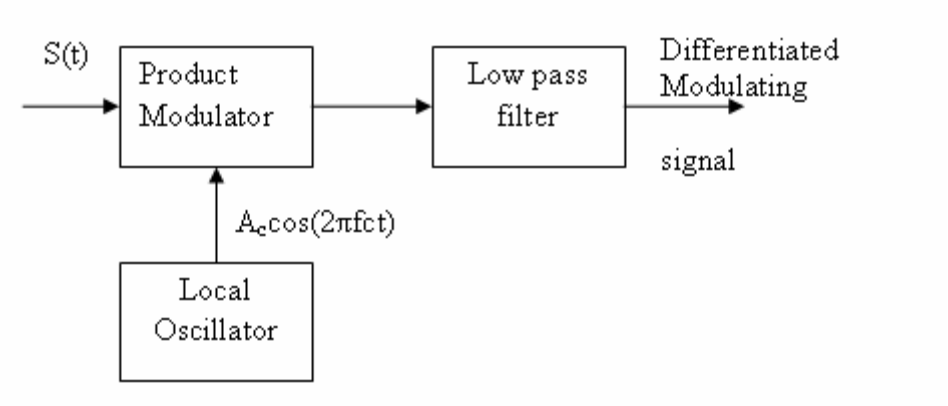

Figure 2-7: Coherent detection of the DSBSC signal

signal and the carrier whose frequency components are located at $2f_c$-f_m and $2f_c$+f_m. The second term is the differentiated modulated signal which has frequency component located at f_m, which is the desired signal. Passing the above signal through a low pass filter with a cutoff frequency at f_m will result in the desired signal.

2.7 Low pass filter

In the above discussed example, as the input modulating signal is a sine wave with frequency f_m, the differentiated signal will also be cosine wave at the same frequency. A random signal, when differentiated, will have frequency components different from that of original signal. Appropriate cutoff frequency is required to design the low pass filter.

Special care also has to be taken when dealing with carrier frequencies which are comparable to the modulating signal. A simple low pass might not remove all the traces of the carrier frequency after it is demodulated. Higher order filters are used in these cases.

The output of the filter is a differentiated modulated signal which should have high signal-to-noise ratio when compared to the signal differentiated at low frequencies.

2.8 Signal-to-noise ratio

The important parameter in the entire process of differentiation and demodulation is the signal-to-noise ratio of the output signal. Signal-to-noise ratio(SNR) can be defined as the ratio of the average power of the message signal to the average power of the noise signal.

A noise free signal is differentiated signal and the signal power is calculated. Later, white noise is added to the input signal and differentiated at low frequency and the corresponding power is measured. The noise power is then measured by subtracting this power from the signal power without any noise. The SNR is calculated from the above obtained values. The SNR improves for amplitude modulated differentiated data

Matlab and PSpice simulations of the above described block diagram are explained in Chapter 3 and Chapter 4 respectively. Experimental results are described in Chapter 5.

CHAPTER 3: MATLAB SIMULATIONS

Simulations in Matlab are performed to verify the results obtained with hand-calculations [7]. These results can also be used as a bench mark during PSpice simulations and actual experiments.

3.1 Sine wave input

Matlab simulations have been performed using the modulating signal of $A_m\cos(2\pi f_m t)$ and carrier signal of $A_c\cos(2\pi f_c t)$. The Fourier transform of amplitude modulated signal has frequency components at *fc-fm* and *fc+fm* with magnitude $(A_c * A_m)/2$.

The transfer function of the differentiator is given by $-RC\frac{dV}{dt}$. It can be designed in Matlab by multiplying the *RC* gain with the slope of the given wave. Its gain increases with frequency of the signal in the time domain. In the frequency domain it has a +20dB slope crossing zero dB at $f = \frac{1}{2\pi RC}$. The value of *RC* determines the zero in frequency domain and also gain to be obtained at other frequencies.

As the gain of the differentiators might be higher that the obtainable in hardware they are decreased by using a decade divider. All the other blocks were also simulated in Matlab using there transfer functions. Filters are accomplished using Matlab functions butter and filter.

Waveforms at each and every stage of simulation and the frequency domain and carrier signal *c(t)* and the frequency spectrums of the same are shown in Figure 3.1(a),(b)

and Figure 3.1(c) and 3.1(d) respectively. The amplitude modulated signal and the corresponding FFT are shown in Figure 3.1(e) and 3.1(f). The frequency components are located at f_c-f_m and f_c+f_m and amplitude of each component will be half the product of the amplitude of carrier and modulating wave. To reduce the amplitude it is further divided by 10 V. This AM signal after passing through differentiator is shown in Figure 3.1(g) and 3.1(h). Observe that different frequency components in the signal are amplified to different magnitudes. The difference in magnitude of the frequency components can be given by A_1-A_2, Eq[2.13(b)]. The amplitude modulation of differentiated carrier and modulating signal are shown in Figures 3.1(i) and 3.1(j). The output of the summer and the corresponding Fourier spectrum is shown in Figure 3.1(k) and 3.1(l). Here the undesired components due to the negative sign difference between them. The only component left after summer is the desired modulated signal. The demodulated signal and its frequency components are shown in Figure 3.1(m) and 3.1(l) This signal can be easily recovered as the difference between f_m and $2*f_c$ is high. The output of the low pass filter is shown in Figure 3.1(o) and 3.1(p).

Matlab simulations have been performed using different modulating and carrier frequencies. Magnitude of resultant waveforms obtained at each and every stage is provided in Table 3.1. The output voltage of the summer is proportional to the $2\pi RCf_mA_cA_m$. The maximum voltage in the circuit results from the differentiation of carrier frequency and it is given by $2\pi f_cA_c$. Both of them depend on the frequency of the modulating and carrier signals. All other terms in the equations are constants. Three major conclusions can be inferred from Table 3.1; namely,

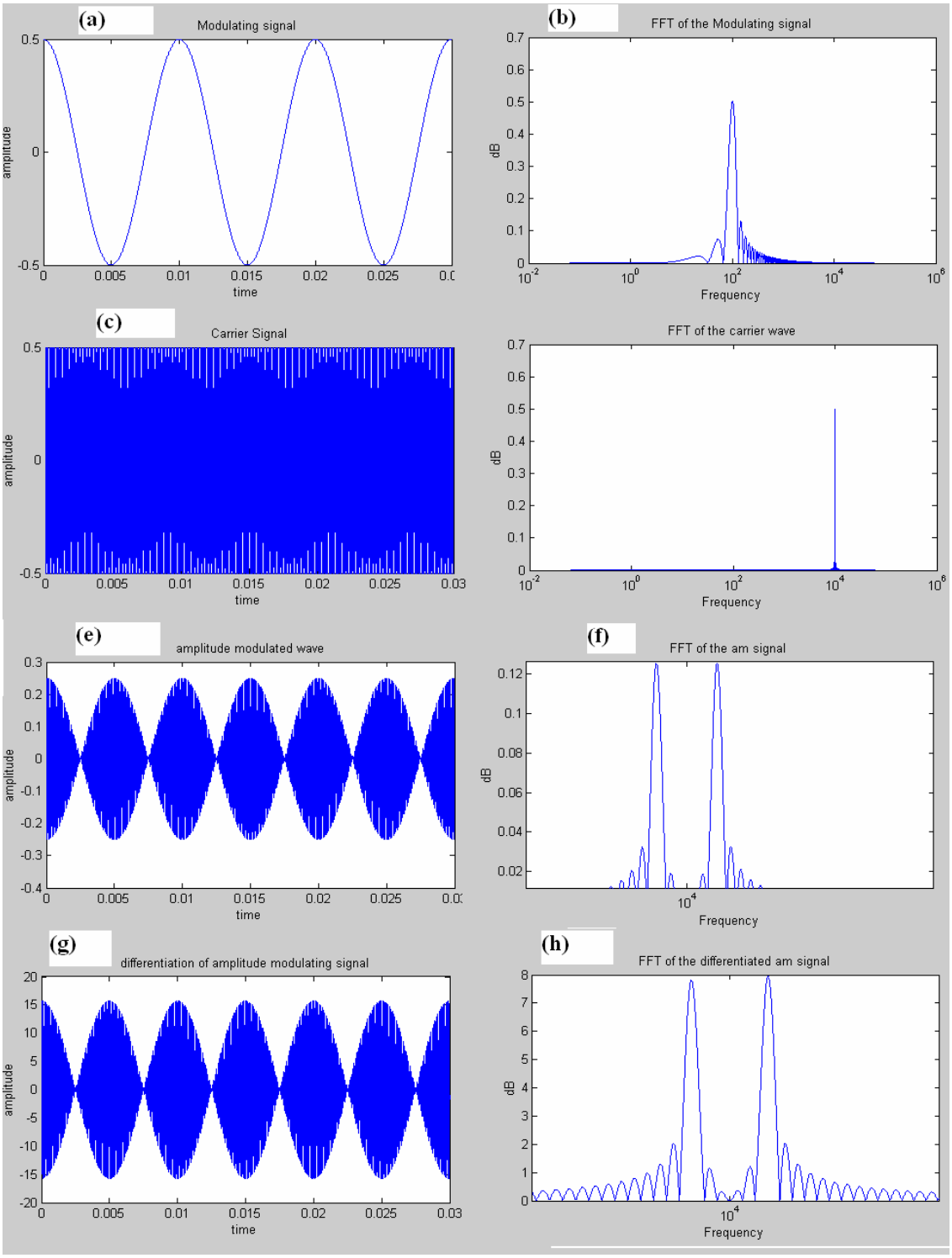

Figure 3-1: (a)Modulating signal (b) Frequency spectrum showing a pulse at 100 Hz (c) Carrier signal (d) FS of carrier wave (e) Amplitude modulated wave (f) Two frequency components at fc-fm and fc+fm (g) Amplitude modulated differentiated signal (h)Frequency components

`

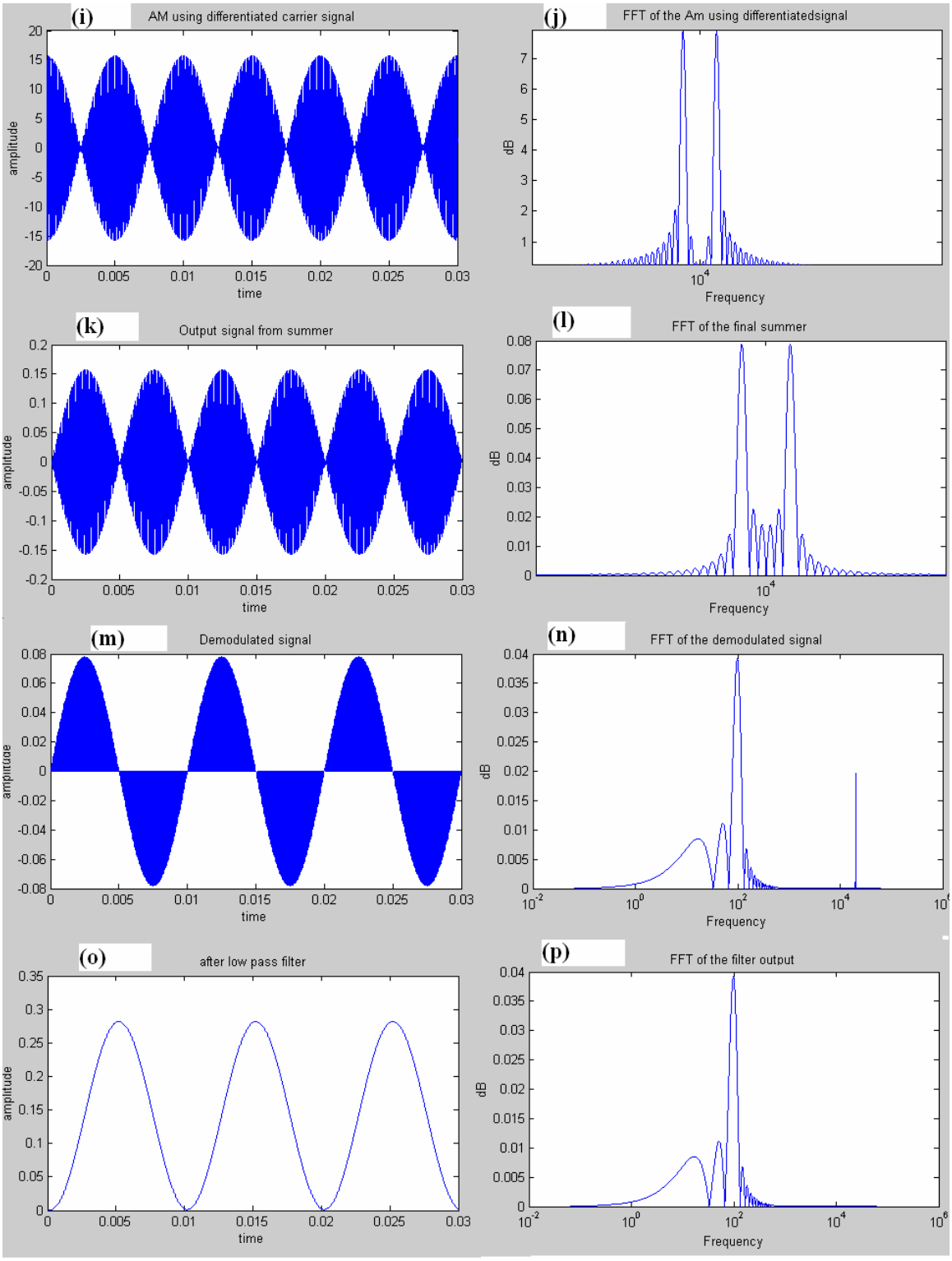

Figure3.1 (i) Amplitude modulation of modulating signal with differentiated carrier (j) Frequency spectrum of the same (k)Output from the summer (l) Low amplitude desired frequency components. (m) Demodulation signal (n) Frequency components of demodulated wave at fm, 2fc+fm and 2fc-fm (o) Filtered differentiated modulating signal (p) Frequency spectrum of filtered signal

`

Table 3-1: Amplitudes obtained of signals during different stages of differentiation

	Modulating signal		Carrier Signal		Diff (RC)	AM	Diff of AM	Diff of Carrier wave	Undesired signal	Summing amplifier (X_1+X_2)	Demod	Output voltage
Units	Freq (Hz)	Amp (V_{pp})	Freq (Hz)	Amp (V_{pp})		Amp (V_{pp})	Amp (V_{pp})	Amp (V_{pp})	Amp (V_{pp})	Amp(V_{pp})	Amp (V_{pp})	Amp (V_{pp})
Magnitude		A_m		A_c	RC	$\frac{(AmAc)}{20}$	$(A_1+A_2)/2 \pm (A_1-A_2)/2$	$2\pi RCf_cA_c$	$(A_1+A_2)/2$	$5(A_1-A_2)$	$((A_1-A_2)A_c)$	A_1-A_2
Frequency components		f_m		f_c		f_c-f_m, f_c+f_m	f_c-f_m, f_c+f_m	f_c	f_c-f_m ,f_c+f_m	f_c-f_m, f_c+f_m	f_m, $2fc$	f_m
	100	16	1k	1	1e-3	0.8 (0.2,0.2)	19.458 (4.5,5.5)	6.123	19.458 (5,5)	2.010 (5,5)	0.9285 (2.4,1.3)	0.4874
	100	16	1k	1	1e-4	0.8 (0.2,0.2)	0.4864 (0.45,0.55)	0.6123	0.4864 (0.5,0.5)	0.0503 (0.05,0.05)	0.0232	0.0122
	100	16	10k	1	1e-4	0.8 (0.2,0.2)	4.8980 (4.95,5.05)	6.123	4.8980 (5,5)	0.0503 (0.05,0.05)	0.0232 (0.024,	0.0116
	100	16	20k	1	1e-4	1	12.24	12.24	12.24	0.0628	0.029	0.0145
	100	16	10k	2	1e-4	0.8	9.7960	12.2459	9.7960	0.1005	0.0929	0.0464
	100	20	20k	2	1e-4	2.4	29.3896 (3.1,3.16)	24.4917	29.3896 (3.13,3.13)	0.1257	0.1161	0.06
	100	16	10k	3	1e-4	3.2	19.5920	24.4917	19.5920	0.2011	0.3715	0.1858

`

1) The output amplitude of the differentiated signal is only dependent upon the modulating frequency f_m and differentiator gain RC as shown in Eq[2.13 b]
2) The output magnitude is limited by with the values of RC as the gain from the differentiated carrier is also dependent of this term, Eq[2.17].
3) The carrier frequency can be increases till the magnitude of the differentiated carrier signal does not cross maximum voltage limit of the op-amp being used in hardware.

The maximum upper limit to the carrier frequency occur when the magnitude of differentiated carrier frequency exceed the op amp output swing limitation. Limit can also be occurred when the output differentiated magnitude is reduced is to a low value.

3.2 Simulated temperature data with noise

Desired differentiated cosine signal is obtained using a sine wave. The signal to noise ration improvement is verified by using a white noise effected simulated temperature data used in [4]. This signal is shown in Figure 3.2; it has a pass band of 100 Hz. This signal is affected with white noise and resultant data obtained using voltage rate sensor interface is shown in Figure 3.3.

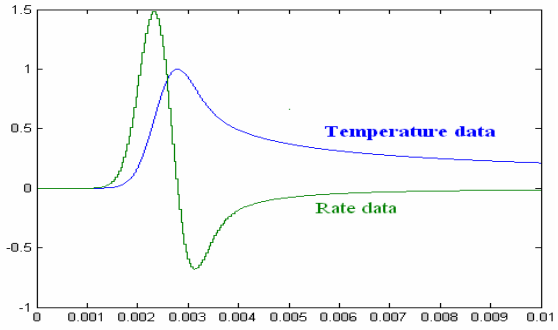

Figure 3-2: Temperature and heating and cooling rate data

`

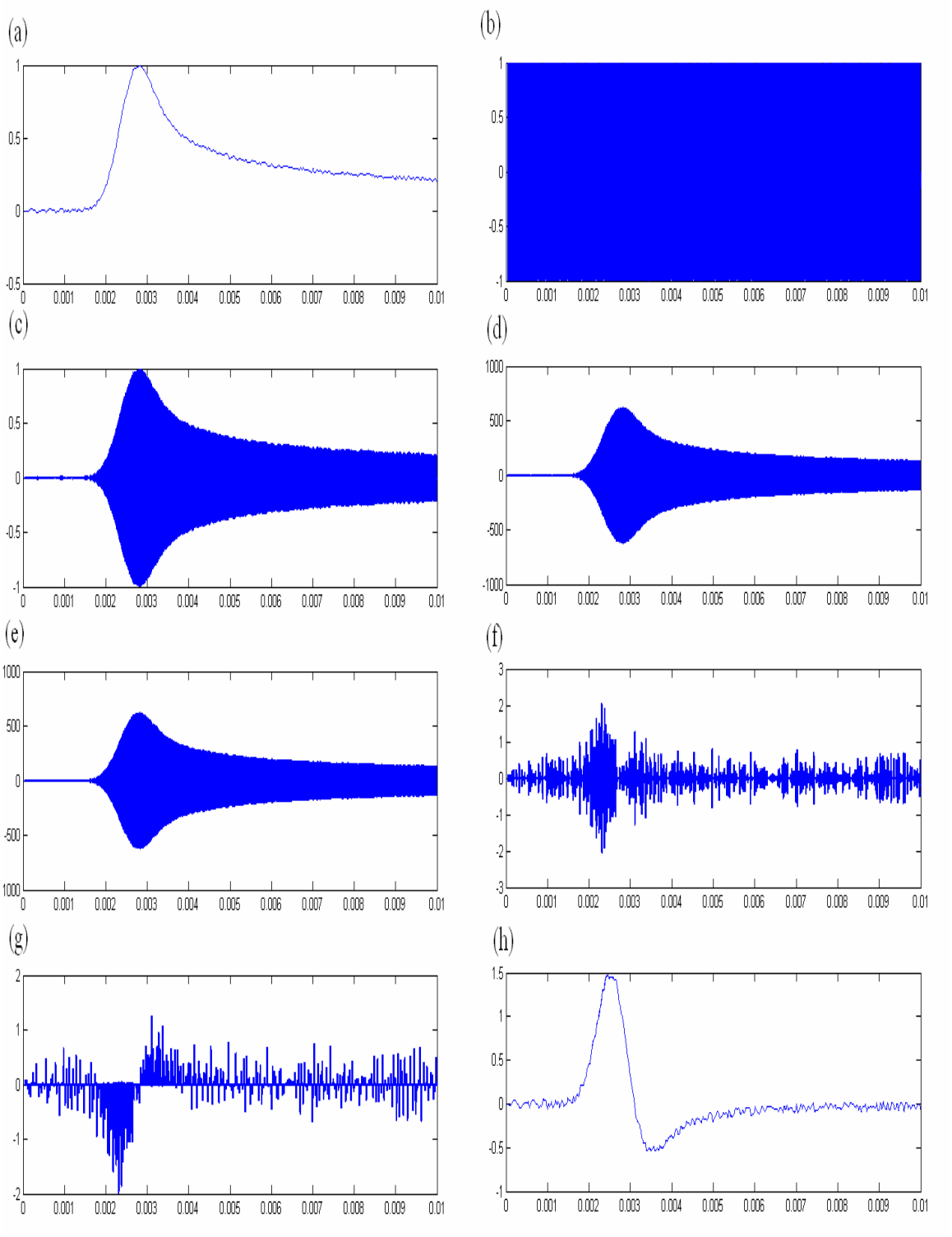

Figure 3-3: (a)Modulating signal (b) carrier signal (c) amplitude modulated signal (d) amplitude modulated differentiated signal (e) amplitude modulated signal using differentiated carrier (f) the output from summing circuit (g) the output from demodulator (h) Demodulated output

`

The output obtained at individual stages of block diagram is shown in Figure 3.3. The noisy temperature data is given as modulating signal is shown in Figure 3.3(a). The carrier signal , amplitude modulated signal, amplitude modulated differentiated signal, amplitude modulated signal using differentiated carrier, the output from summing block, the output from demodulator, and the final results obtained after passing through a low pass filter are shown in Figure 3.3 (b)-(h) respectively.

Figure 3.4 shows the results of when the noisy signal is differentiated at low frequency. Due to the noise present in the input signal, the obtained output signal will be noisy and unreliable. The signal-to-noise ratio obtained is also low. The output obtained when differentiating at high frequencies by using amplitude modulated differentiation is shown in Figure 3.5. The results match the results obtained when the signal is differentiated without any noise. SNR of the signal improves with increase in carrier frequency. Table 3.2 shows the SNR obtained using different carrier frequencies.

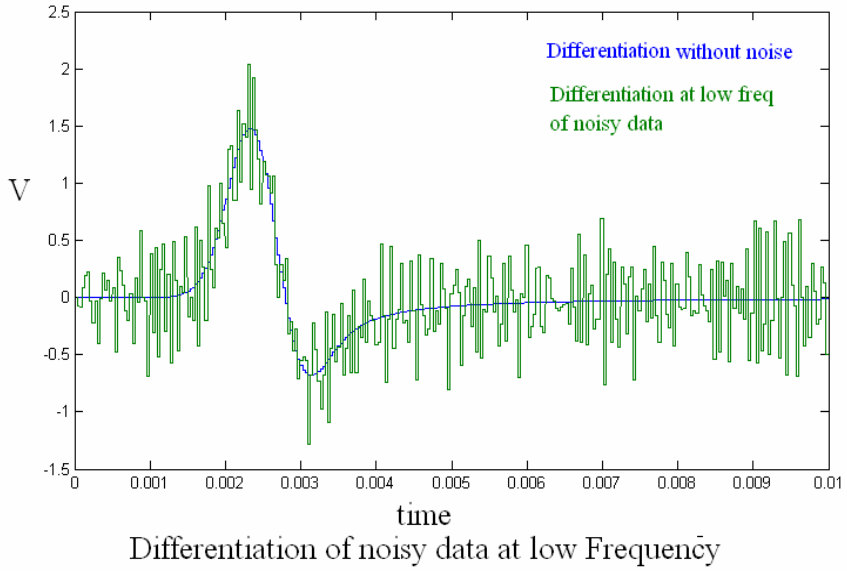

Figure 3-4: Differentiation of temperature data at low frequency

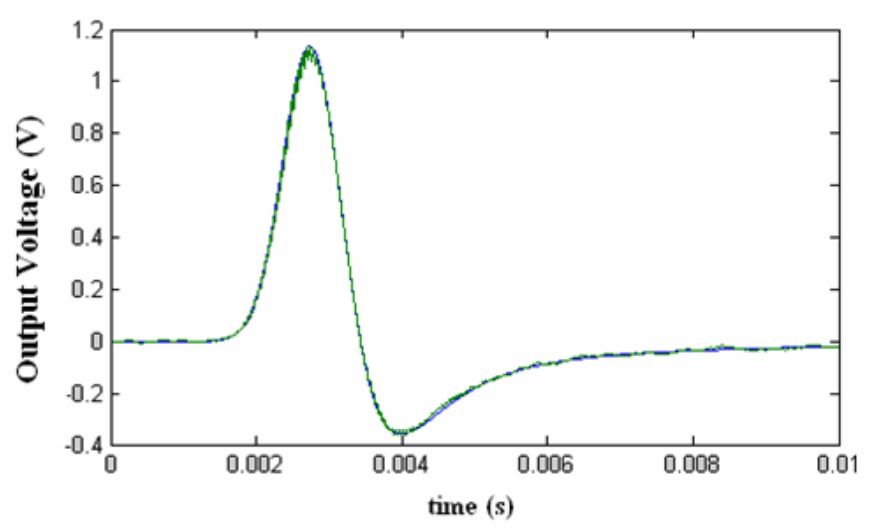

Figure 3-5: Differentiation of temperature data at high frequency

Table 3-2: SNR obtained using different carrier frequencies obtained from Matlab

SNR of noisy signal differentiated at low frequency	SNR of filtered signal differentiated at low frequency	Carrier frequency (Hz)	SNR of noisy signal differentiated at high frequency	SNR of filtered signal differentiated at high frequency
10.29	48.4420	10k	44.4697	23.9883
10.29	48.4420	20k	351.6670	48.3164
10.29	48.4420	30 k	141.9521	81.4681
10.29	48.4420	40k	54.0662	119.9552
10.29	48.4420	50k	73.9511	173.9028
10.29	48.4420	60k	73.4499	240.1650
10.29	48.4420	70k	262.0165	343.3325
10.29	48.4420	80 k	94.58	468.0271
10.29	48.4420	90k	61.8925	753.4291
10.29	48.4420	100 k	46.86	1205.02
10.29	48.4420	110 k	54.54	2220.8

`

The signals are sampled at the rate of 1920100 samples per second. The signal-to-noise ratio at low frequency is 10.2 This can be increased to 1205.2 by amplitude modulating with a carrier frequency of 100k and differentiating at this higher frequency. Figure 3.6 shows the improvement in SNR with increase in carrier frequency. Figure 3.6 also shows the improvement in signal-to-noise ratio with increase in sampling rate due to the decreases in RMS error with increases in sampling rate.

The circuits used to simulate each block of the Figure 2.6 are explained in detail in chapter 4. Design requirements and simulation results are also explained in detail.

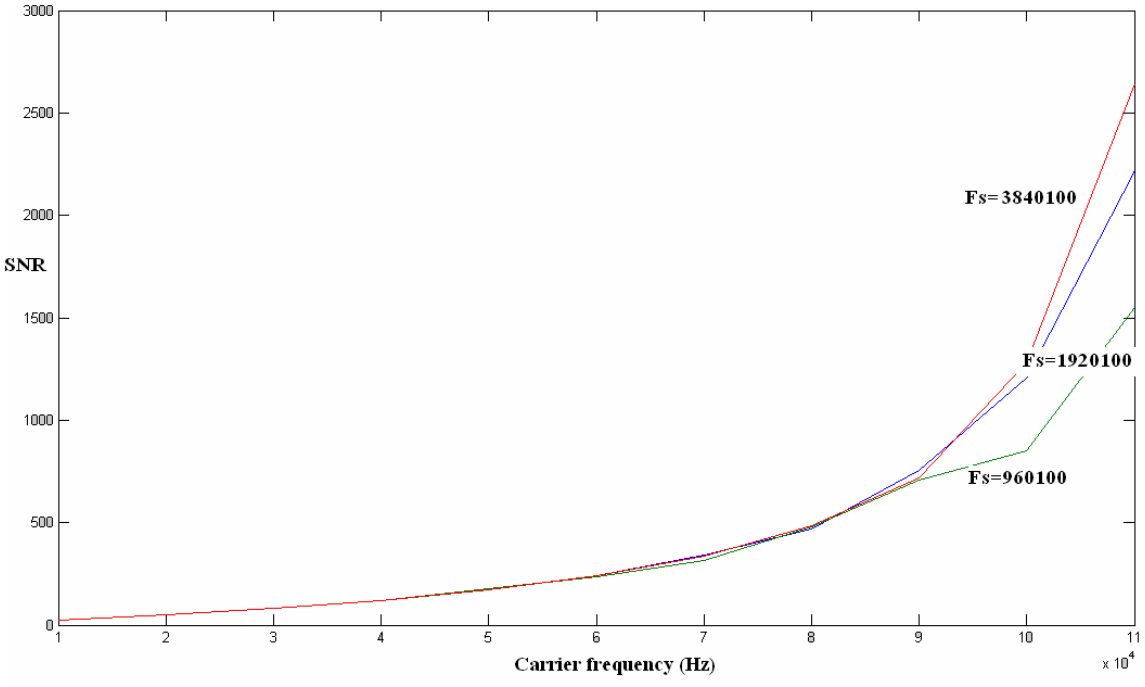

Figure 3-6 : SNR with increase in carrier frequency

CHAPTER 4: PSPICE SIMULATIONS

Prior to constructing a circuit, careful design is required using simulation software. All the electrical simulations are performed in PSpice. PSpice (Simulation Program with Integrated Circuit Emphasis)[8] is analog circuit simulation software that runs on personal computers, hence the first letter "P" in its name.

Each part of the block diagram shown in Figure 2.6 is explained in detail in this chapter. The design requirements and the parts used are explained in detail. The Simulation results are provided when required. The main components required in the experiment are oscillator, for creating the carrier signal, low pass filters for filtering the input signal and demodulated signal; multiplier for modulating and demodulating the signal and differentiator for differentiating both carrier and amplitude modulated signal. Each block is explained in detail in the following sections.

4.1 Oscillator

An electronic oscillator produces periodic signal at regular interval of time. Voltage controlled oscillator (VCO) is a form of harmonic oscillators which produce sine wave whose frequency can be varied by the applied DC voltage. This is used to produce the carrier wave required for modulation.

If the frequency of oscillations has to be varied across a large range of frequencies, varactor diode is used. The change in capacitance of the reverse biased varactor diode due to applied voltage will cause the change in oscillation frequency. The oscillation frequency of the voltage controlled oscillator is stabilized using a Phase Locked Loop (PLL). PLL will correct the error frequency during oscillations by feeding

its output back to the input signal and producing an error signal. This error signal produces an error correcting DC voltage which helps in locking the oscillations to a particular frequency.

The IC in which oscillations from VCO are controlled in a PLL is EXAR XR2206 [9], which can also be used as function generator. The block diagram and pin configuration of the chip is shown in Figure 4.1. The frequency of oscillation can be changed from 0.01Hz to 1MHz with an external control voltage applied, while maintaining low distortion. It also has excellent temperature specifications of 20ppm/^{o}c.

XR2206 is capable of producing two independent frequencies. The four main functional blocks in XR2206 are VCO, current switches, sine shaper, and unity buffer amplifier. The VCO output is dependent on the voltage at the timing resistors which can be controlled using current switches. The distortions in the oscillation can be removed using external adjustments in the sine shapers block. Unity buffer amplifier is used to avoid loading effects on the output of VCO.

The frequency of oscillation from the VCO is proportional to the current through the timing pins at 5,6,7,8. A fixed capacitor(C) is placed between pins 5 and 6 and two timing resistors (R_1, R_2) at pins 7, 8 to produce two different output frequencies. The frequency of oscillation is determined mainly by the variable resistors at pin 7 and 8 and is given by

$$f_{c1} = \frac{1}{R_1 C}, \quad and \quad f_{c2} = \frac{1}{R_2 C}. \qquad [4.1]$$

If pin 9 is open circuited or connected to a bias voltage greater than 2V, R_1 is activated. But if the voltage is less than 2V, R_2 is activated. As we need only one carrier

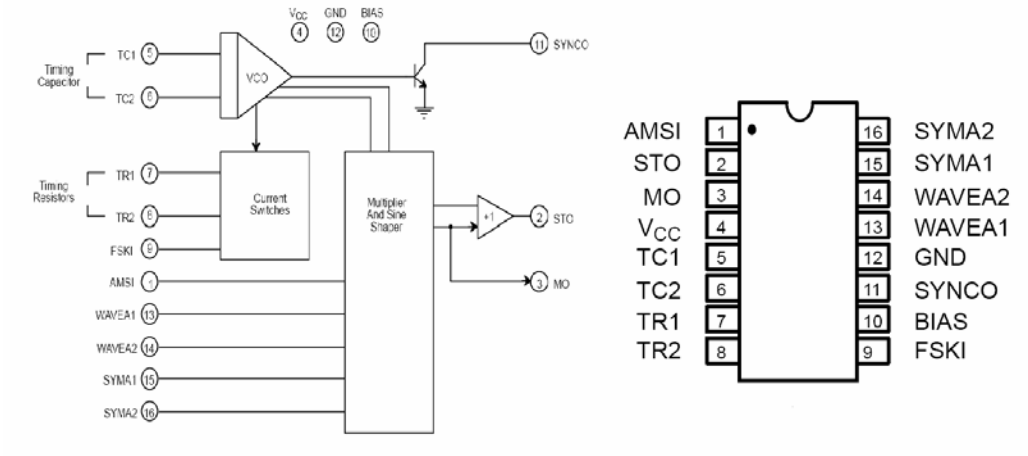

Figure 4-1: (a) Internal Block diagram and(b) pin configuration of XR2006(taken from [9])

frequency to generate the AM signal, we only use timing resistor at pin 7. This oscillator can be operated in either single supply configuration or split supply. If used in single supply configuration the output DC voltage will depend on the voltage at pin 3. Split supply is used during simulation to achieve a zero output dc voltage.

The configuration used for producing a carrier frequency is shown in Figure 4.2. It uses external symmetry adjustment available for removing any distorting present in the input. The potentiometer R1 at pin 7 provides frequency tuning. If the symmetry adjustment is not used there will be a distortion less than 2.5%. With symmetry adjustment this distortion can be further reduced to 0.5%.

Resistor R_A and R_B are used for symmetry adjustment. R_A is used to adjust the sine shaping resistor in the multiplier and sine shaping block. R_B is used for fine adjustments in the waveform symmetry. The steps to be followed for adjustment are as follows

1.Set R_B at midpoint and adjust R_A for minimum distortion

2.With R_A set as above, adjust R_B to further reduce distortion

`

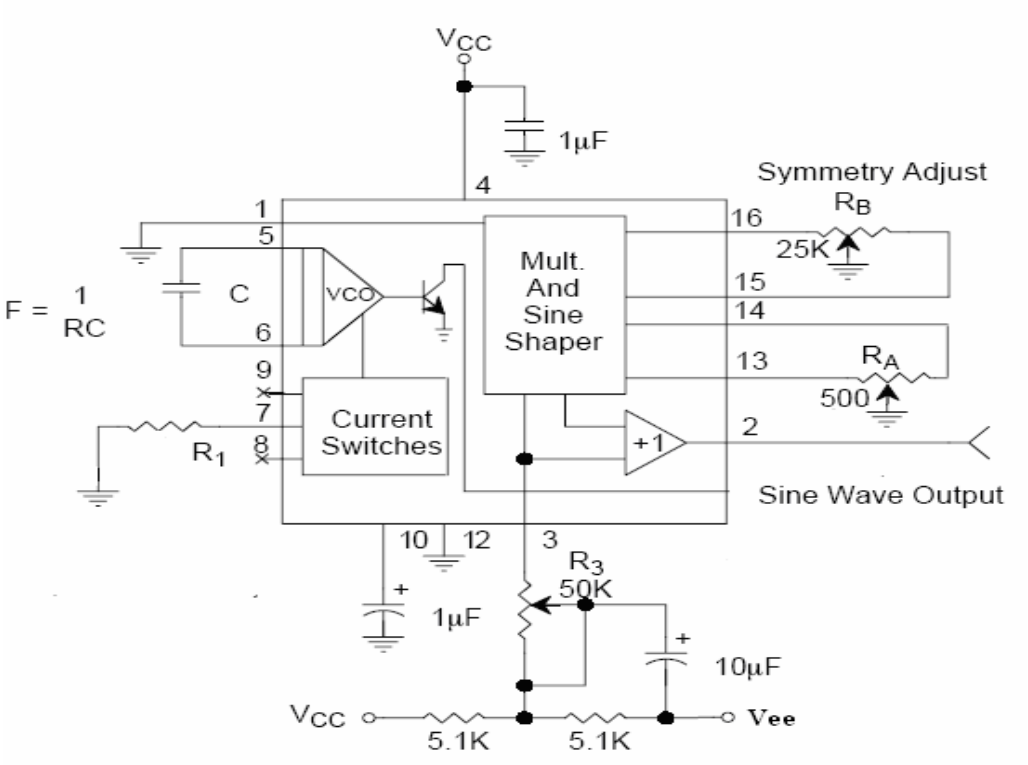

Figure 4-2: Sine wave generation with minimum harmonic distortion

4.2 Low Pass Filter

A filter is a frequency selective network that allows a certain range of frequencies to be passed and reject other frequencies. A low pass filter can be realized using a RC network. Using only passive elements in designing a filter has limitation of quality factor, Q, of the filter is limited to ½. A filter is said to have a high *Q* if it selects or rejects a narrow range of frequencies compared with its centre frequency. *Q* can be obtained by dividing the central frequency by 3dB bandwidth.

To obtain a higher Q value, we use active filters, i.e. using an amplifying element such as an operational amplifier along with the passive elements. The order of the filter determines how steep the frequency curve falls from pass band to the stop band. For every pole added to the circuit, an additional +20dB slope is added to the curve.

`

The schematic of the Sallen-Key low pass filter[10] is shown Figure 4.3. At low frequencies both the capacitors are open circuited so the input is directly transferred to the output. At high frequencies both the capacitors are short circuited so the signal does not appear at the output. But at the cutoff frequency of the filter when impedance of C_1 and C_2 is equal to impedance of R_1 and R_2, the positive feedback through C2 will help improve the quality factor of the circuit. The transfer function of the above circuit can be derived as follows.

Gain of non inverting input is given by

$$k = 1 + \frac{R_f}{R_g} \qquad [4.2]$$

The voltage developed at the negative terminal of the op-amp is given by

$$k = \frac{V_{out}}{V_{in}} \qquad [4.3]$$

If the voltage at node 3 is V_3 then the output relation between the output voltage and input voltage can be written as

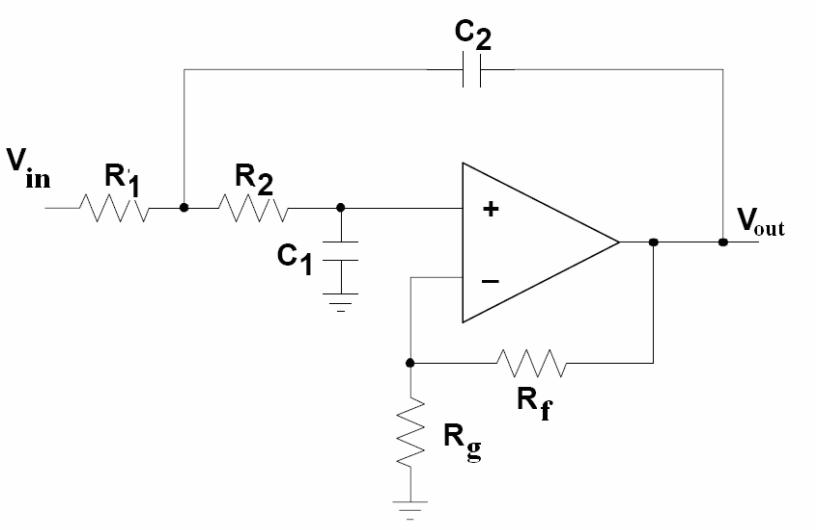

Figure 4-3: Sallen-Key low pass filter

`

$$\frac{V_3 - V_{in}}{R_1} = \frac{V_{out} - V_3}{\frac{1}{sC_1}} + \frac{V_3 - V_{in}}{R_2} \qquad [4.4]$$

The relationship between V_3 and V_{in} can be written as

$$V_3 = V_{in}(1 + sR_2C_2) \qquad [4.5]$$

Substituting Eq[4.5] in to Eq[4.4], we find

$$Vout = \frac{\frac{K}{R_1R_2C_1C_2}}{s^2 + \left(\frac{1}{R_1C_1} + \frac{1}{R_2C_1} + \frac{1}{R_2C_2}(1-k)\right)s + \frac{1}{R_1C_1R_2C_2}} \qquad [4.6]$$

From the Eq[4.6] we can define the cutoff frequency of the filter to be

$$\omega_c = \sqrt{\frac{1}{R_1R_2C_1C_2}} \qquad [4.7]$$

and the quality factor of the system as

$$\frac{1}{Q} = \left[\left(\frac{R_2C_2}{R_1C_1}\right)^{1/2} + \left(\frac{R_1C_2}{R_2C_1}\right)^{1/2} + (1-k)\left(\frac{R_1C_1}{R_2C_2}\right)^{1/2}\right]$$

The design is greatly simplified by using R_1=R_2=R and C_1=C_2=C and the cutoff frequency reduces to

$$fc = \frac{1}{2\pi RC} \qquad [4.8]$$

and quality factor of

$$Q = \frac{1}{3-K} \qquad [4.9]$$

The disadvantage of using this configuration is that quality factor is dependent on the gain *k* of the circuit. If a better quality factor is required we have to increase the gain by cascading two filters with increasing gains.

`

4.2.1 Design

Careful design is required for not adding any additional delay in the circuit. Delay is caused due to the phase shift between input and output waveform. The phase shift between input and output starts a decade before the pole actually occurs in the frequency domain. The phase of the signal at the pole frequency is 45 degrees and it reaches 90 degrees after crossing it. To avoid any phase shift, the cutoff frequency of the filter is chosen a decade after the actual pole present in the system. The frequency range of the heat transfer signals range from 0 Hz to 100 Hz. The cutoff frequency of the filter chosen is 1 KHz.

Choosing the value of capacitor to be 0.1 μf and using Eq[4.8] the value of resistor is equal to $R_1=R_2=1.59$ KΩ for cutoff frequency of 1 KHz The filter designed after demodulation of the differentiated signal should have a cutoff frequency that is greater than the cutoff frequency for modulating signal. Figure 4.4 shows the difference in spectrum of the temperature and rate data. The cutoff frequency of the filter after demodulation is above 1500 Hz.

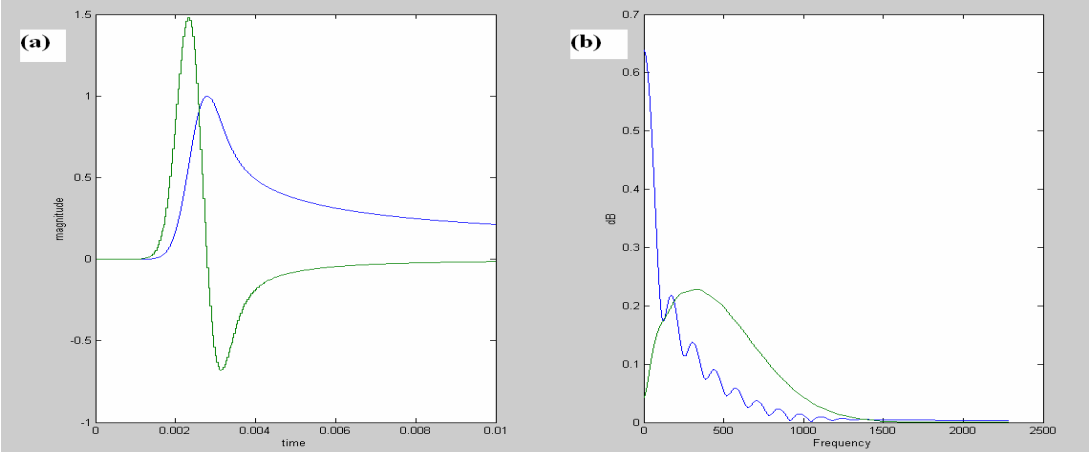

Figure 4-4: (a)Temperature and rate data (b) Frequency spectrum of the same

`

4.2.2 Simulation results

In the experiment, filtering is performed on a low frequency signal, hence the bandwidth required for the op amp is not very high. The experiment also requires that offset voltage to be low. The op amp chosen for this block is op-27 which has an offset voltage which is less than 10 µf and is also unity gain stable. The frequency response of the circuit used in Figure 4.3 is shown in Figures 4.5. The -3 dB point of the circuit is at 1 KHz . From the frequency response, all the frequency components below 100 Hz are passed without any phase shift. Frequency components between 100 Hz and 1 KHz are passes with some phase shifted. All the other frequencies are attenuated. The Butterworth filter used also ensures zero ripples in the stop band.

4.3 Differentiator

An op-amp circuit whose output is proportional to the rate of change of the input signal is called a differentiator. Its schematic is shown in Figure 4.6.

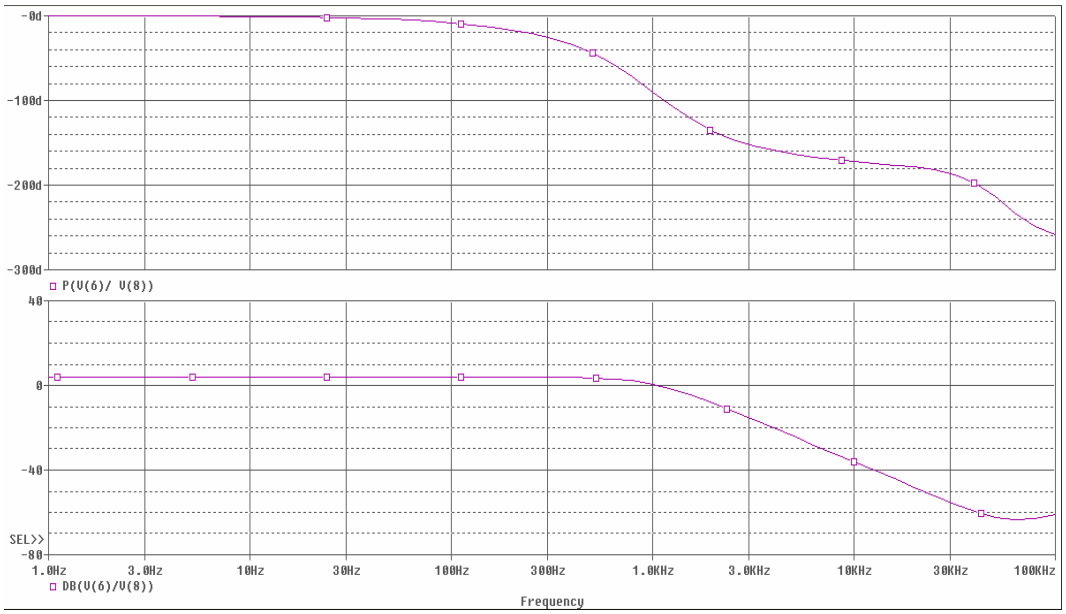

Figure 4-5: Frequency response of low pass filter

`

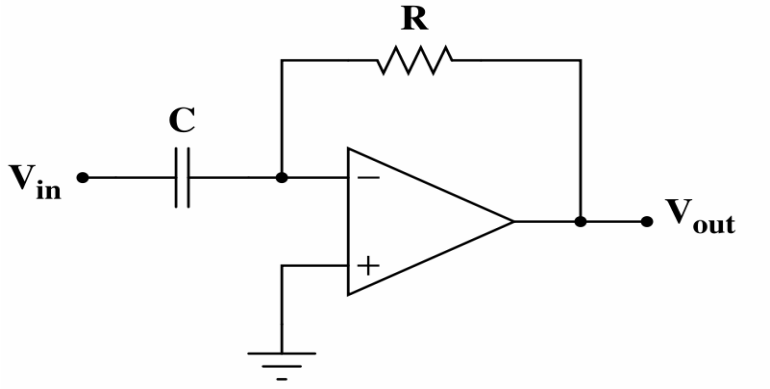

Figure 4-6: Schematic of simple differentiator

The positive terminal is at ground so the voltage of the negative terminal is also at ground due to effect of virtual grounding. The current *I* that flow in capacitor C is

$$I = c\frac{dv}{dt} \qquad [4.10]$$

The current is thus proportional to the rate of change in the input voltage. If the input voltage changes at a rapid rate, the current produced increases correspondingly. The current flowing into any terminal of an ideal op-amp is zero. Thus the entire current from the capacitor has to flows into the resistor.

$$C\frac{dV_{in}}{dt} = -\frac{V_{out}}{R} \qquad [4.11]$$

$$V_{out} = -RC\frac{dV_{in}}{dt} \qquad [4.12]$$

as an inverting op amp configuration is used the output will have a negative sign. The frequency response of a simple differentiator is shown in Figure 4.7. Its gain crosses zero dB when it encounters the zero of the circuit. The location of zero is calculated using

$$f_c = \frac{1}{2\pi RC} \qquad [4.13]$$

`

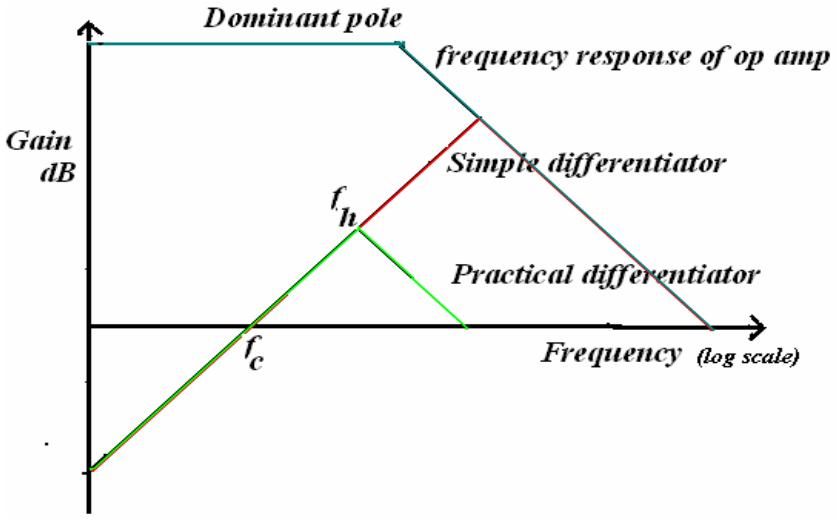

Figure 4-7: Frequency response of simple and practical differentiator

This circuit is not suitable for practical applications. At high frequencies, the gain of the circuit increases as the capacitor is short circuited. This results in a larger amplification of the noise component in the input signal. Also, the R and C loop acts as a low pass filter and provide a 90 degree phase shift to the input signal which results in resulting in a total phase shift greater than 180 degrees. As the phase shift is 180 degrees the op amp is be positive feedback amplifier which is undesired.

4.3.1 Practical differentiator

The circuit in Figure 4.8 is used as differentiator for all practical purposes [11]. Resistor R_1 is added in series with the differentiating capacitor C_1 near the negative input terminal and a capacitor C_2 is added in parallel to the feedback resistor R_2. Adding these additional RC pair converts the differentiator into an integrator at high frequencies. Also at high frequencies, when both the capacitors are short circuited, the gain is limited to $-\frac{Rf}{R1}$ due to the series resistance.

`

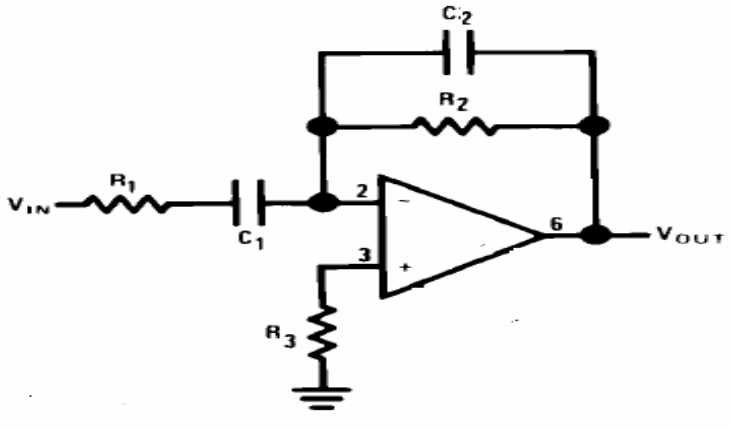

Figure 4-8: Practical differentiator

Current flowing through resistor R_1 and capacitor C_1 branch is

$$I = \frac{V_{in}}{R_1 + \frac{1}{sC_1}} \qquad [4.14]$$

neglecting the voltage at the negative input terminal, the equation for output voltage of the op amp is

$$V_{out} = -I.(R_2 \parallel \frac{1}{sC_2}) \qquad [4.15]$$

substituting Eq[4.14] in the above equation

$$V_{out} = -\frac{V_{in}}{R_1 + \frac{1}{sC_1}}.(R_2 \parallel \frac{1}{sC_2}) \qquad [4.16]$$

Solving Eq[4.16], and substituting $s=j\omega$

$$\frac{V_{out}}{V_{in}} = -\frac{\frac{j\omega}{R_2C_1}}{(1+\frac{j\omega}{R_1C_1})(1+\frac{j\omega}{R_2C_2})} \qquad [4.17]$$

The above equation has a zero and two poles. When $R_1C_1=R_2C_2$, two poles will overlap giving a + 40dB change in the slope at the pole frequency.

`

The zero in Eq[4.17] is given by

$$f_Z = \frac{1}{2\pi R_2 C_1} \qquad [4.18]$$

f_Z is the frequency where the gain of the differentiator crosses zero dB. The intersecting poles are at frequency f_h

$$f_h = \frac{1}{2\pi R_1 C_1} = \frac{1}{2\pi R_2 C_2} \qquad [4.19]$$

f_h is the frequency where the gain of differentiator is maximum. After f_h the circuit acts as an integrator. The relation between these two frequencies is

$$f_Z \leq f_h$$

Using an additional *RC* pair adds two additional poles to the circuit and limiting the high frequency gain thus attenuating high frequency noise. In addition, R_1C_1 and R_2C_2 form lead networks in the feedback loop which, if placed below the amplifier unity gain frequency, provide 90° phase lead to compensate the 90° phase lag of R_2C_1 and prevent loop instability.

4.3.2 Design

The design of differentiator is the most important part in the entire block diagram. This differentiator is used in two different instances in the circuit, i.e. for differentiating both carrier and amplitude modulated wave. The carrier is a single frequency component wave f_c, but the amplitude modulated wave is the sum of two individual bands of frequencies that are located on either side of carrier frequency f_c.

As the signal to be differentiated has frequency components around the carrier frequency, f_Z is designed to be smaller than the f_c to achieve a gain higher than 0dB at the

desired frequency range. Also the maximum frequency component in amplitude modulation given by f_c+f_m should be less than the maximum gain of the differentiator. To avoid any additional delays because of the phase shift introduced by the poles, f_h must be a more than $10(f_c+f_m)$.

The magnitude of the output voltage, given in Eq[2.17], for the entire circuit is determined by the differentiator. Thus the major limitation while designing the differentiator is the gain of the circuit at the modulating frequency f_m. This can be explained using Figure 4.9. If the gain at the modulating frequency is small as shown in Figure 4.9 (b), the output signal cannot be retrieved. There is no limitation on the value of carrier frequency.

If we design the gain of the differentiator at f_m to be large as shown in Figure 4.9 (a), the differentiated output wave can be retrieved. There will be limitation on carrier signal frequency, as the op amps used cannot deliver the higher gains attained at such frequencies. This is explained much better in Table 4.1.

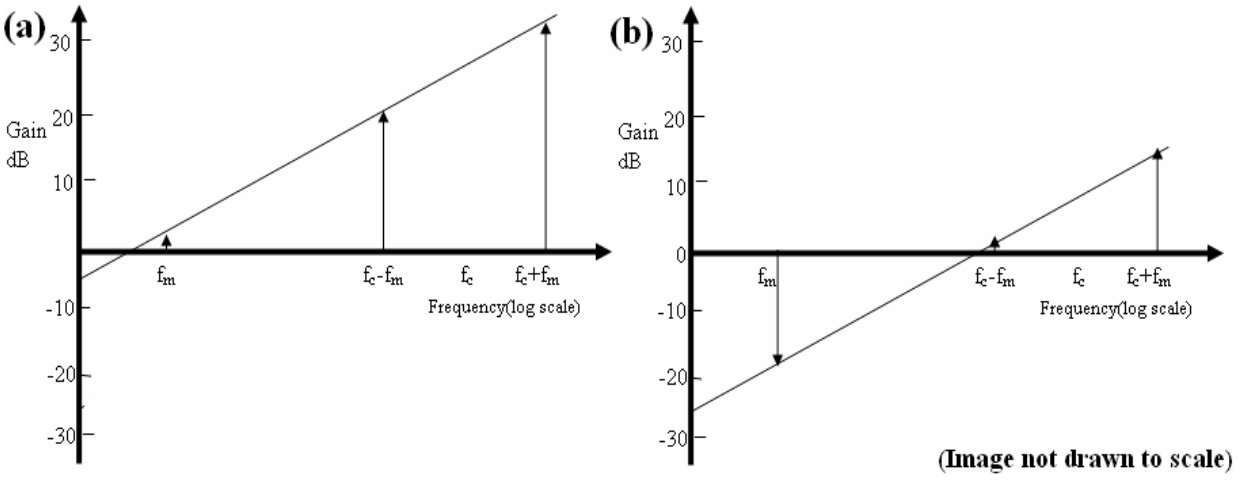

Figure 4-9: Effects of zero in differentiator design

`

Table 4-1: Magnitude at every stage obtained using two different differentiator

Input/Output Signals	Equations	Magnitude (V_{P-P}) fC = 10 KHz, $\mathbf{R_2C_1 = 1e\text{-}4}$	Magnitude (V_{P-P}) fC =10 KHz, $\mathbf{R_2C_1 = 1e\text{-}3}$
Modulating signal	Am	20	20
Carrier signal	Ac	1	1
Differentiated carrier signal	$2\pi RCfcAc$	6.28	62.8
Amplitude modulated signal	$(AmAc)/20$	1	1
Differentiation of AM signal	A_1 $(A_1+A_2)/2,(A_1-A_2)/2$	6.28 (3.10,3.17)	62.8 (62.17,63.4)
AM signal using differentiated carrier	A_1 $(A_1/2, A_1/2)$	6.28 (3.14,3.14)	62.8 (31.4,31.4)
Output from summing amplifier	A_1-A_2	0.06	0.6
Demodulator	A_1-A_2	0.06	0.6

`

The value of R_2C_1 determines the location of where magnitude of the output signal crosses 0dB in frequency domain. Table 4.1 explains the tradeoff between the magnitude of the differentiated modulated signal obtained at the end of the process and the maximum carrier frequency that can be used which determines the signal-to-noise ratio of the output. If the magnitude of the output signal is low, it cannot be retrieved properly. Similarly if the SNR is low, the output signal cannot be differentiated from noise signal

The position of zero in the frequency domain for the circuit determines the output magnitudes. If the zero is near the modulating signal the output voltage is high with low SNR. However, if the zero is near the carrier frequency, the output magnitude is low with an excellent SNR. Table 4.1 is used to determine the values of R_2C_1 and the carrier frequency used in the experiment.

4.3.3 Simulations

PSpice simulations have been performed using different carrier and input signal values. Figure 4.10 shows the frequency response of the differentiator. An op 27 op amp

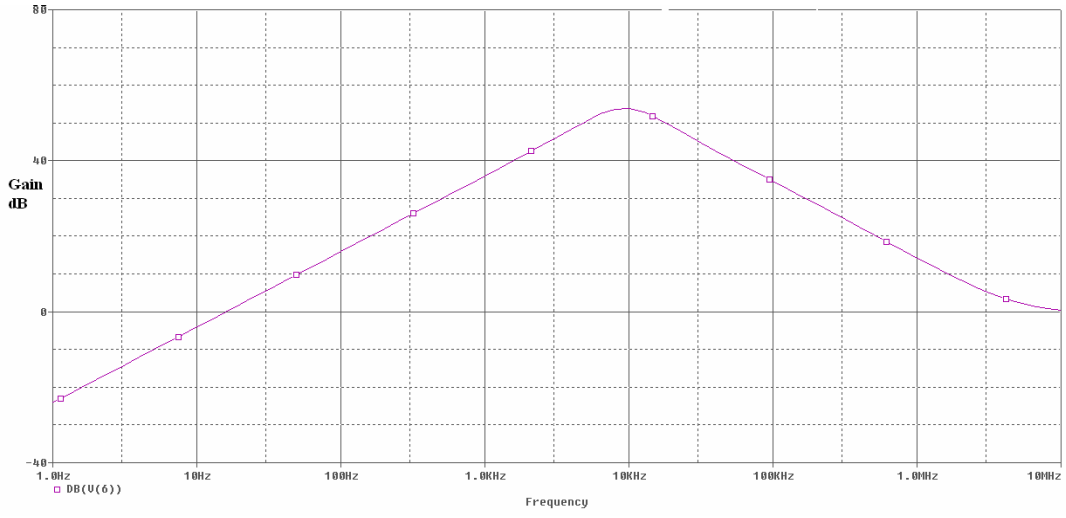

Figure 4-10: Frequency response of the differentiator

`

is used for simulation where R_1= 10 Ω, C_1 = 1 μf, R_2 = 10 kΩ and C2= 1 ηf. The zero of the system is located at 16 Hz, so the gain for a low frequency signal will be greater than unity. The overlapping poles are located at 16 KHz. The highest carrier frequency that can be used for this experiment with out any additional phase delay in the output is around 6 kHz. Higher carrier frequency can be applied by shifting the position of the zero and poles of the circuit.

The time response of the above circuit is shown in Figure 4.11. Sine wave input will result in an amplified cosine wave output. The circuit is also verified with different input waves

4.4 Multiplier

Multiplier is also one of the most important parts in the entire process of amplitude modulation differentiation. It is used in both modulation and demodulation methods. The op amp used to perform this task is an AD633 [12], which is a four quadrant multiplier. The block diagram is shown in Figure 4.12.

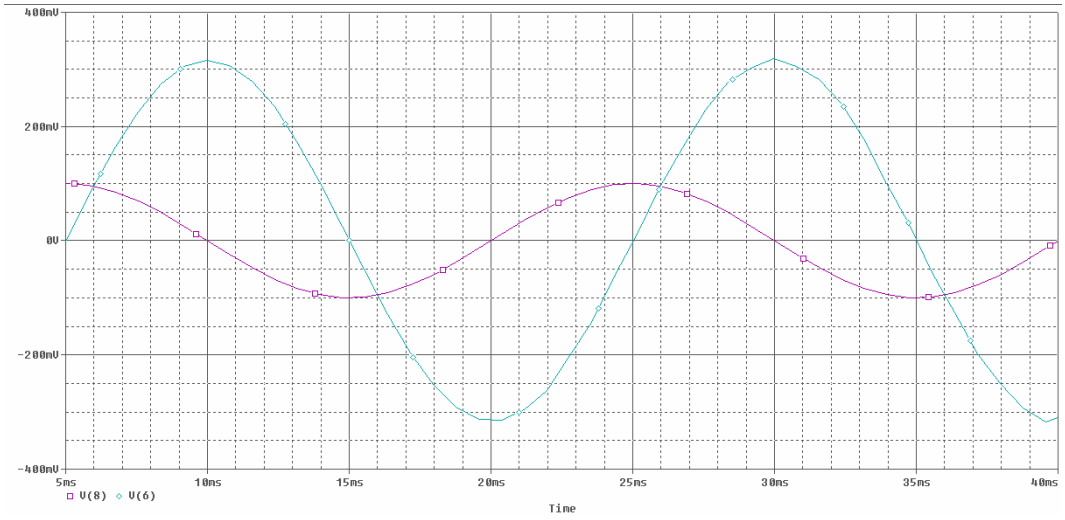

Figure 4-11: Time response of differentiator

`

The two high impedance differential input pairs, X and Y, are useful in making loading negligible. These inputs are multiplied and the product is full scaled by 10 V using a buried zener diode to increase the output swing.

The output from this multiplier can be added to the signal (Z). The output of the op amp is

$$Vout = \frac{(X_1 - X_2)(Y_1 - Y_2)}{10} + Z \qquad [4.20]$$

This op amp has a bandwidth of 1 MHz, slew rate of 20 μV/V and noise less than 100μ which are desired for the required operation. It can also operate on dual power supply ranging from ±8 V to ±18 V.

When two voltage inputs are given as inputs at terminals X and Y, they are first converted into differential currents by using voltage to current converters. The product of these currents is then generated using the multiplier core. A two quadrant multiplier [13] is one where only one signal can be of double polarity but the other is limited to single polarity. This can be generated using an emitter coupled pair driven by a current mirror. The multipliers will only works in two quadrant of the XY plane. This cannot be used in communication applications like modulation and demodulation.

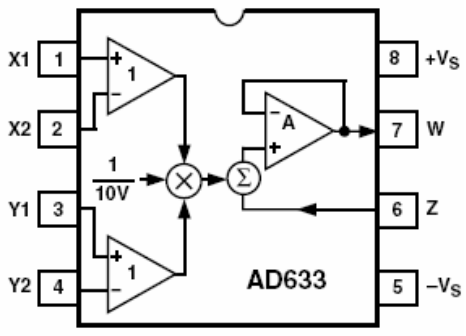

Figure 4-12:Functional block diagram of AD633 (taken from [12])

`

To generate a four quadrant multiplier we have to use a Gilbert's cell which is modification of the emitter coupled pair with balanced multiplier system. The AD633 is a four quadrant multiplier.

The summing node is connected to the carrier input to produce an AM wave without suppressing the carrier. To obtain a DSBSC waveform the summing terminal Z has to be grounded. If the amplitude of the output signal has to be increase, output voltage can be feedback through terminal Z using voltage divider. The configuration used for amplitude modulation is shown in the Figure 4.13. The same configuration can be used for demodulation process by replacing the modulating signal with the modulated signal.

4.4.1 Simulation

The results of PSpice simulation of the amplitude modulator is shown in Figure 4.14. A sine wave carrier with an amplitude of 1 V is used an input. The output has an internal divider of 10, so a modulating signal with amplitude to 10 V is applied as other input signal. The output voltage is a amplitude modulated signal with a amplitude of 1 V obeying Eq[4.20]. Demodulation can also be done using the same setup, and later filter to obtain the desired differentiated signal.

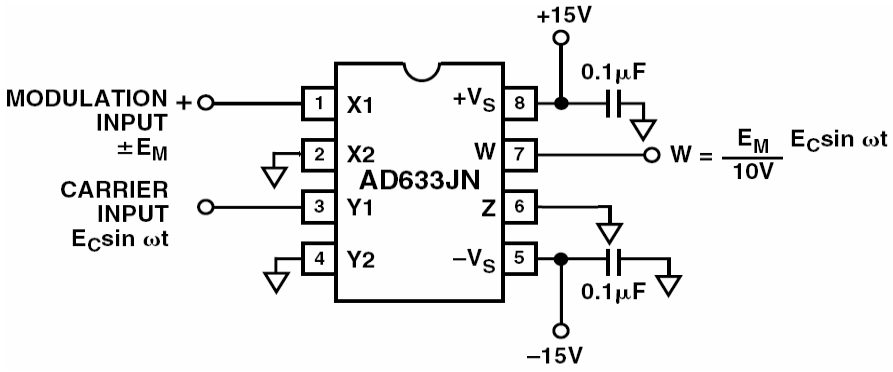

Figure 4-13: Double side band suppressed carrier Amplitude Modulation

`

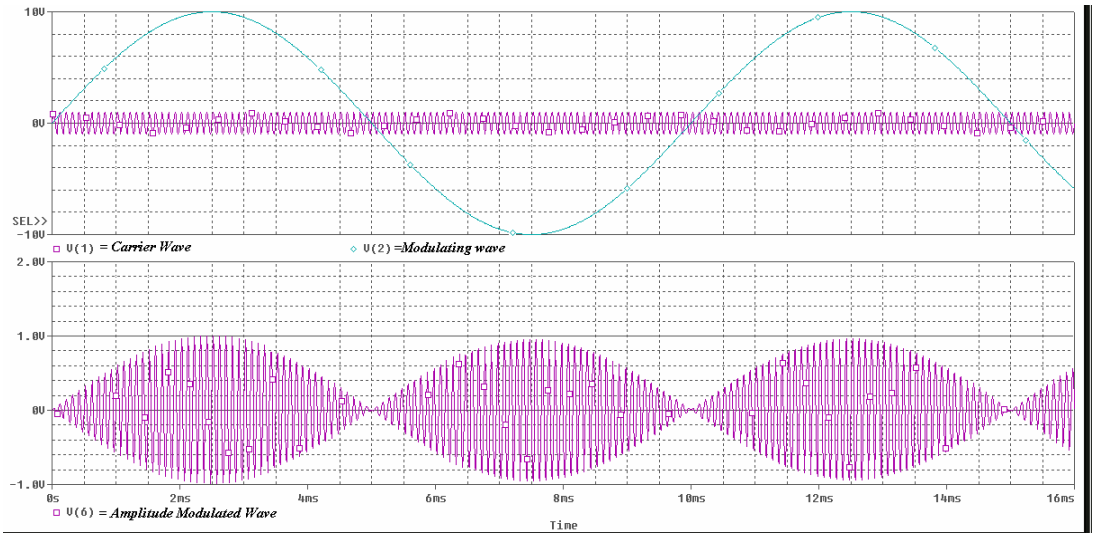

Figure 4-14: Simulation of amplitude modulated signal (a) Both carrier and modulating signal. (b) Amplitude modulated signal

4.5 Summing Amplifier

Summing amplifier is used to add any two signals. It is used in the block diagram to remove the unnecessary components from the modulated differentiated signal. Undesired signal which is out of phase is produced from differentiating the carrier wave and amplitude modulating it with the temperature data. The output obtained when these signals are added contains only desired frequency component.

We have to use a non inverting summing amplifier, as we do not want any phase shift in the output signal. The configuration used for non inverting amplifier is shown in Figure 4.15. Inputs V_1 and V_2 are applied to the positive input terminal of the op amp. The gain of the circuit is given by $\left(1+\frac{R_f}{R_g}\right)$ where R_f is the feedback resistors and Rg is the resistance at negative terminal. The transfer function of Figure 4.15 is derived using super position theorem. If we assume that only V_1 is applied at a given time and V_2 is grounded the voltage the positive terminal can be given as

`

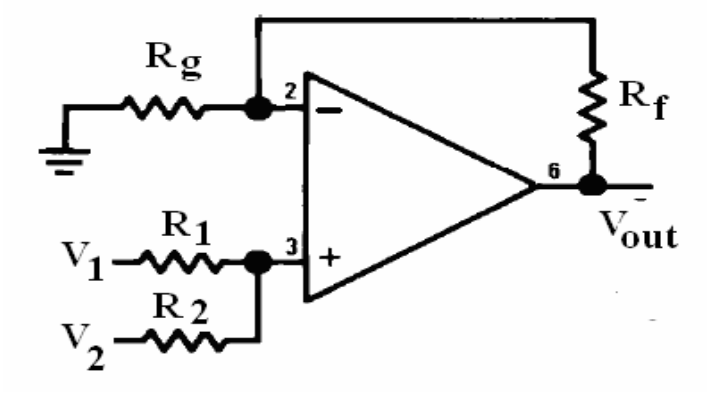

Figure 4-15: Summing amplifier

$$V_{+,1} = V_1 \frac{R_2}{R_1 + R_2} \quad [4.21]$$

similarly, the voltage at the positive terminal due to V2 assuming that V1 is grounded is

$$V_{+,2} = V_2 \frac{R_1}{R_1 + R_2} \quad [4.22]$$

The total sum of voltages at the positive terminal will be given by

$$V_+ = \frac{(V_2 R_2 + V_1 R_1)}{R_1 + R_2} \quad [4.23]$$

The output voltage is given by the main multiplied by the voltage at positive terminal

$$Vout = \left(1 + \frac{R_f}{Rg}\right)\left(\frac{V_2 R_2 + V_1 R_1}{R_1 + R_2}\right) \quad [4.24]$$

If $R_1=R_2=R_f=R_g$ then the output is

$$V_{out}=V_1+V_2 \quad [4.25]$$

The output of the summing amplifier will vary from the sum of the two voltages due to offset voltage of the op amp. An op amp of very low frequency has to be chosen for the implementation. This op amp should also a band width above the carrier frequency used in amplitude modulation. OP-27 [14] is used due to its bandwidth of 8 MHz and offset

voltage of 3 μV. This offset is removed by applying a DC voltage at the input terminal. This can be applied using a variable resistor between the power supplies.

The simulation of the summer adding two signals is shown in Figure 4.16. Two sine wave signals of 100 Hz and 100 KHz are added to obtain the output.

4.6 Buffer Amplifier

When output of one circuit is used as an input to the other circuits, the preceding circuit does not affect the outputs of the succeeding circuits. If a circuit is driving an unknown load, the output voltage will vary according to the load resistance it sees at that output node. If the load resistance is very low, the output varies as the current drawn from the circuit is large. Loading is caused when the output of a circuit is affected by the preceding circuit. Loading can be caused when the circuit is driving a filter or differentiator where the output is across a capacitor. The current drawn from the capacitor will discharge the capacitor, reducing the voltage. Loading can also happen when the op amp is driving another op amp with negligible input resistance [15].

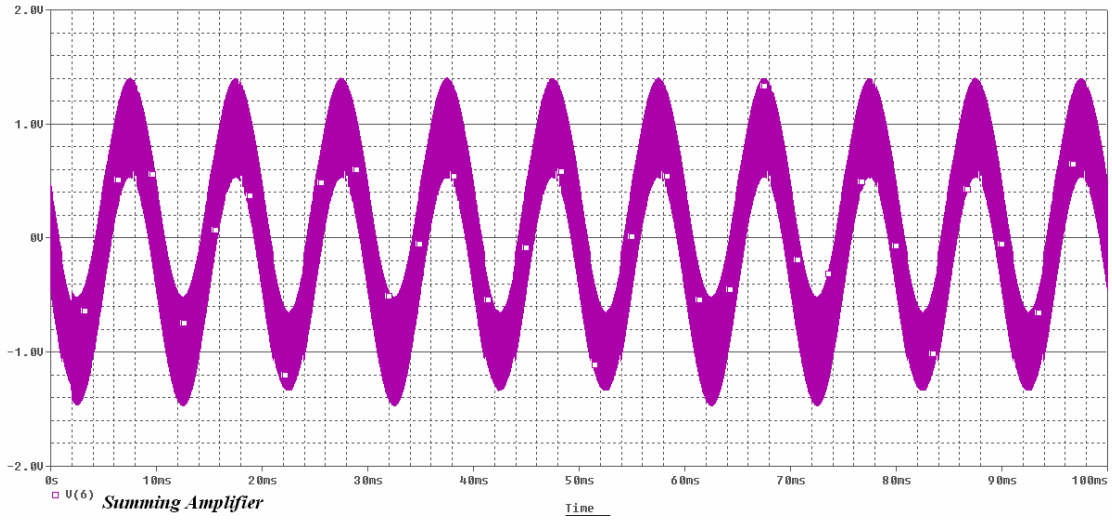

Figure 4-16: Time response of the summing amplifier

`

A buffer amplifier isolates the output of one system from the input of the other, thus avoiding loading. The circuit for buffer amplifier is shown in Figure 4.17. It copies the input from one stage and reproduces it as an input to the preceding stage. It does that without drawing any current from wherever the input voltage terminal is attached. However, at the output terminal can draw whatever amount of current the operational amplifier can supply.

4.7 Complete circuit

The complete electrical circuit of universal voltage rate sensor interface is shown in Figure 4.18. The output measured after integration of complete circuit matches the results obtained during Matlab simulation. Offset adjustment circuits [16] are used before the summing amplifier to get accurate results.

The modulating signal is amplified to a magnitude of 20 Vp-p and filtered using a low pass filter. This is amplitude modulated with a carrier signal of 2 Vp-p. The obtained AM signal and the output after differentiating it are shown in Figure 4.19. The outputs of the differentiating the carrier and AM found using it are shown Figure 4.20. The outputs of the summer where the undesired components cancel each other and the demodulating the summer output are shown in Figure 4.21. The output obtained after filtering the demodulated signal is shown in Figure 4.22. The magnitude of the output differentiated voltage is small and should be amplified.

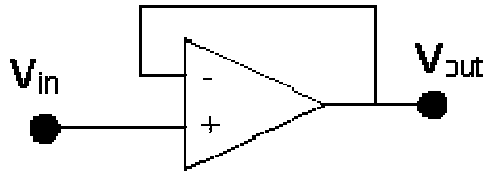

Figure 4-17: Buffer circuit

`

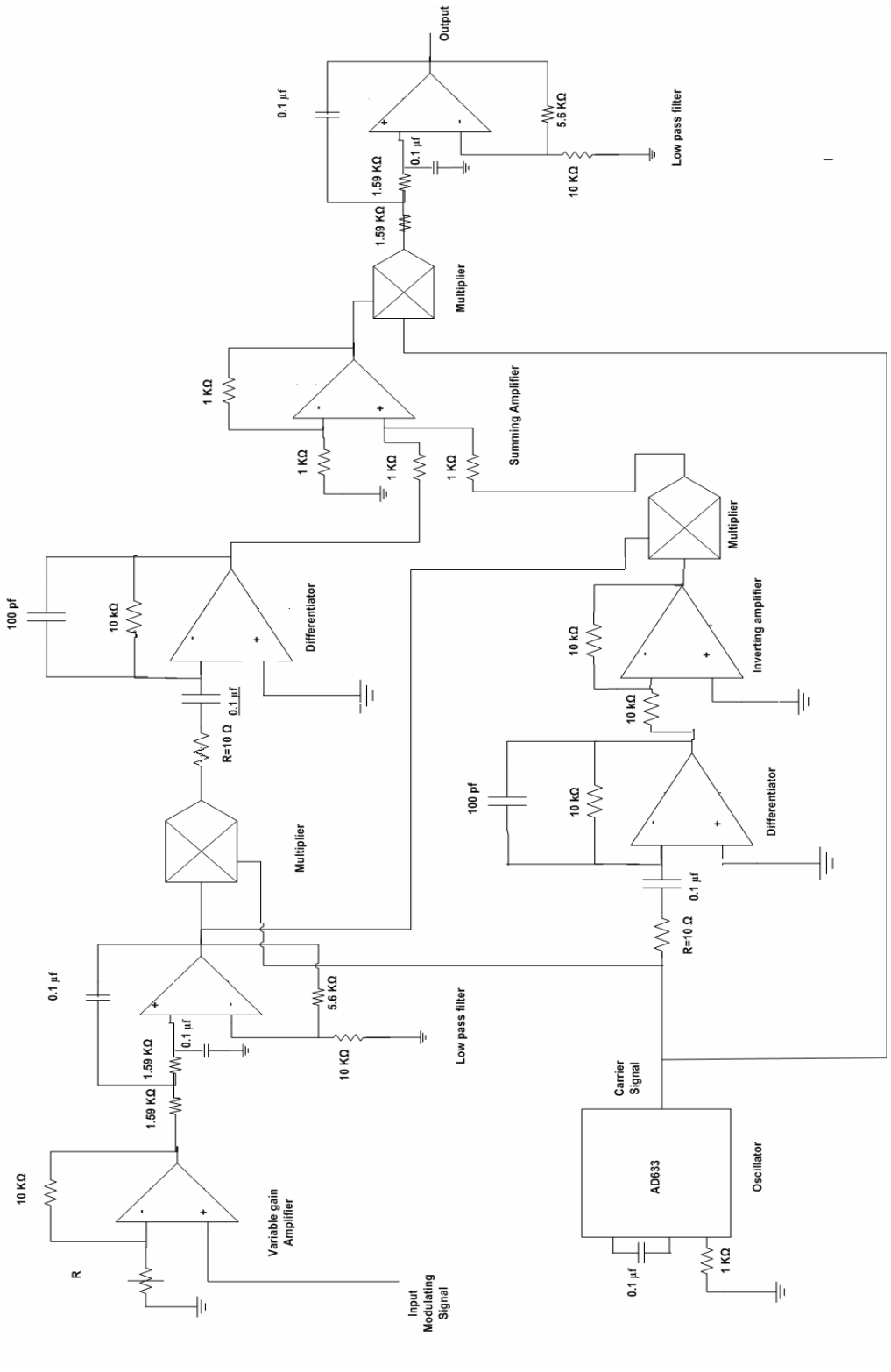

Figure 4-18: Complete circuit of the universal voltage rate sensor

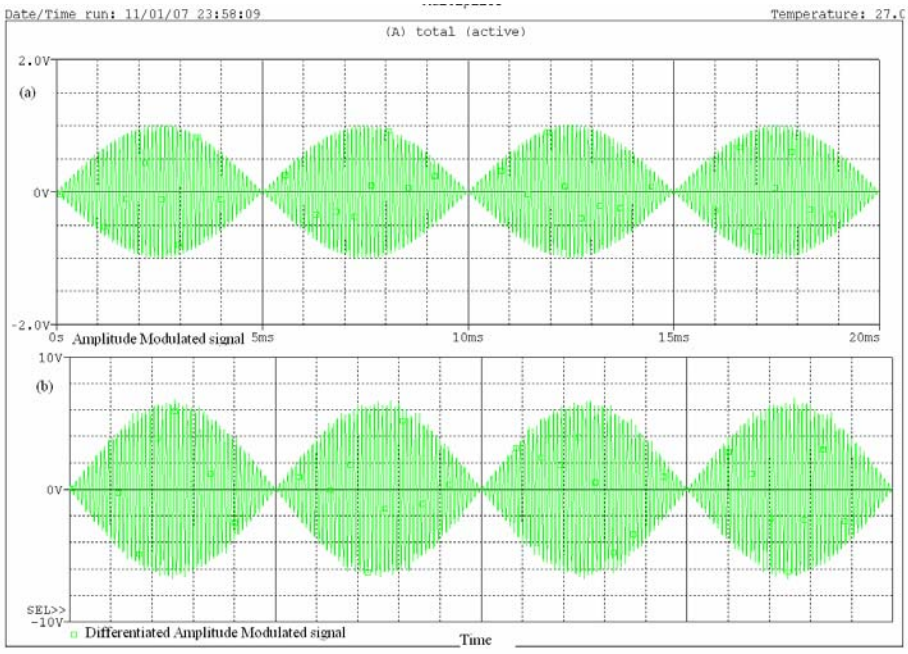

Figure 4-19: Amplitude modulated and Differentiated Amplitude modulated signal

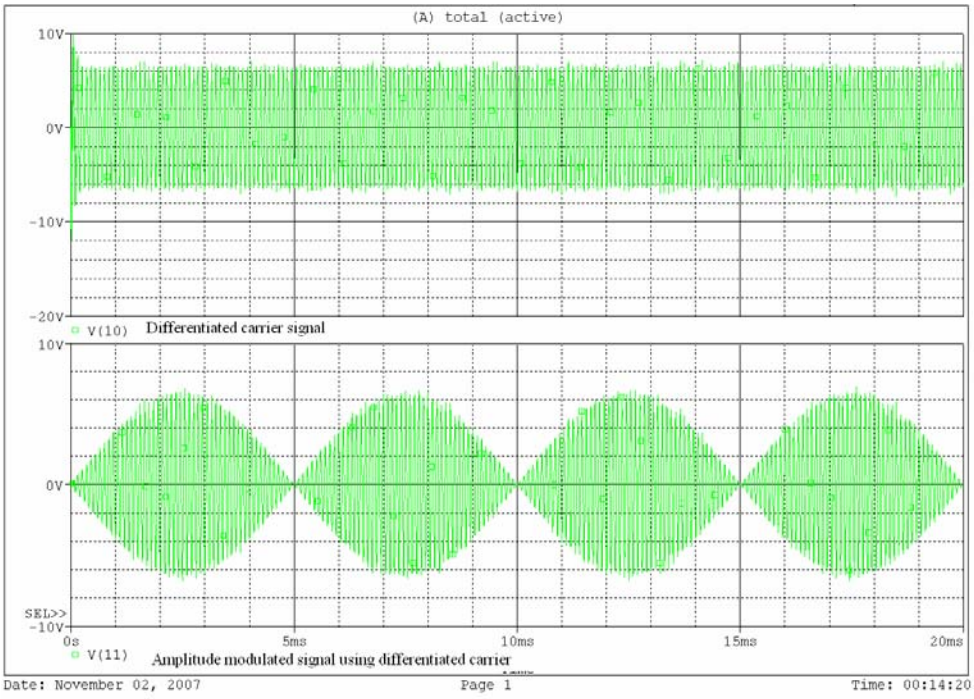

Figure 4-20: Differentiated carrier signal and AM using differentiated of carrier signal

`

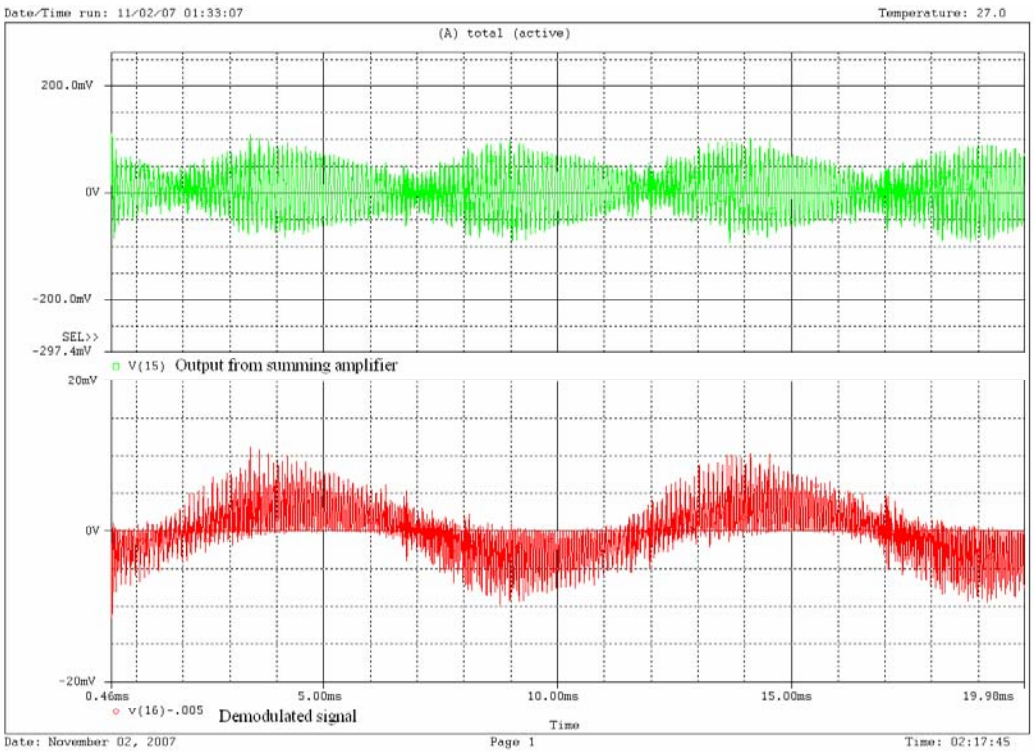

Figure 4-21: The output from the summer and the demodulated signal

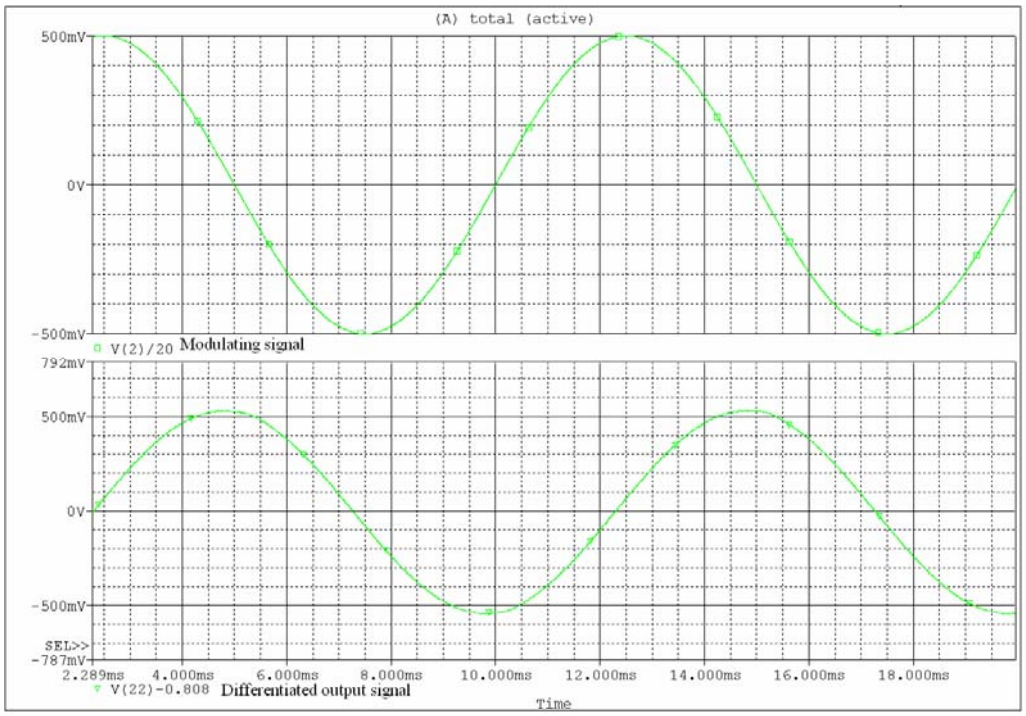

Figure 4-22: The modulated signal and the obtained differentiated carrier signal

`

The Signal to noise ratio improves showing the similar trend shown in Table 3.2 As both Matlab and PSpice simulation show an improvement in signal-to-noise ratio, the experiment are performed and the results obtained a discussed in Chapter 5.

CHAPTER 5: EXPERIMENTAL RESULTS

This chapter provides the results obtained at individual stages of building of the circuit and the final results after integration. These results are then compared with the results obtained in Matlab and PSpice simulations.

For measuring the signal-to-noise ratio, white noise is added to the simulated temperature data. This signal is given as input to the amplitude modulated differentiator. The signal-to-noise ratio of the output obtained from the experiments does not match the results obtained from the simulations. This is due to the additional noise present from the electronics components during the actual experimental procedure. The following precautions were taken to reduce external noise which affects the SNR. Long wires which act as antennas attracting unwanted signals are avoided. Noise from the power supply branches is avoided using a filter at every supply node.

5.1 Analysis

The temperature data is read from a text file and is used produce a periodic input waveform to the sensor interface. The data in the file consists of discrete values belonging to a single aperiodic cycle. When these discrete values are to be transformed into a continuous set of periodic values, the problem of discontinuity arises at beginning of each cycle. This discontinuity between the consecutive cycles leads to the emergence of sharp pulses when differentiated. This problem is overcome by using an averaging program in Matlab. Thus, the discrete aperiodic values are transformed into a periodic set of values using Matlab.

The output text file of the Matlab is fed to an Agilent waveform generator[17]

which generates a continuous waveform. The amplitude and frequency of the input data is changed after the waveform is loaded into the computer. This is very useful when high values of temperature data have to be normalized and given as voltage signals.

The results obtained from the circuit are measured using an Agilent oscilloscope. The output is also stored into the computer using scope probe software provided by Agilent [18]. Data is collected at a sampling rate of 1200 samples/ time scale of the oscilloscope. This is a disadvantage when measuring amplitude modulated signals where higher sampling rate is required to measure both the carrier and modulated wave in a single time scale. In order to acquire data at a higher sampling rate, LabView[19] interface is used in the relevant cases. Frequency spectrum of the signal acquired is also measured using the oscilloscope.

Frequency analysis of the circuit is performed using Sleuth analyzer[20]. Both magnitude and phase of the circuit in a given frequency range is measured.

5.2 Waveforms

The outputs obtained at individual stages of the analysis are presented in this section. Figure 5.1 shows the carrier frequency generated using XR2206 with a magnitude of 1 Vp-p and frequency of 10 KHz. The output frequency is changed using variable resistor.

The frequency response of the low pass filter measured using the sleuth analyzer is shown in Figure 5.2. The gain of the filter is 1.8 with its 3 dB frequency at 1 KHz. The low frequency modulating signal of 100 Hz with a magnitude of 10 V p-p is shown in Figure 5.3.

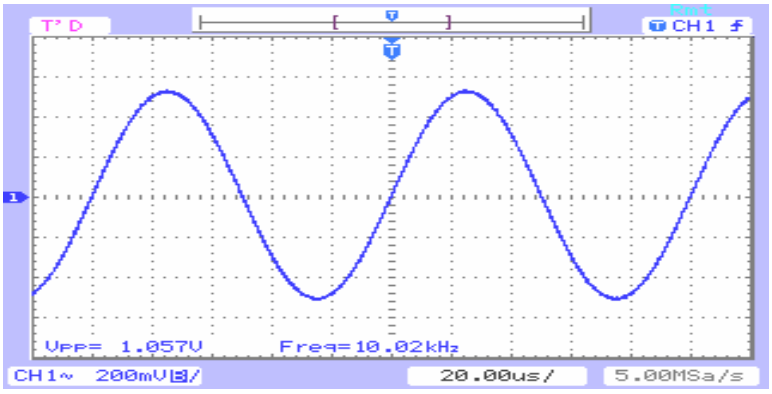

Figure 5-1: Carrier wave generated using XR2206

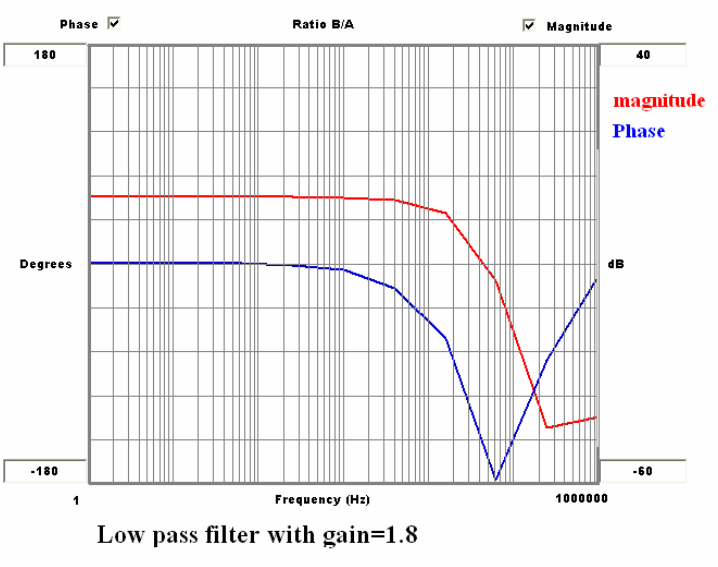

Low pass filter with gain=1.8

Figure 5-2: Frequency response of the low pass filter

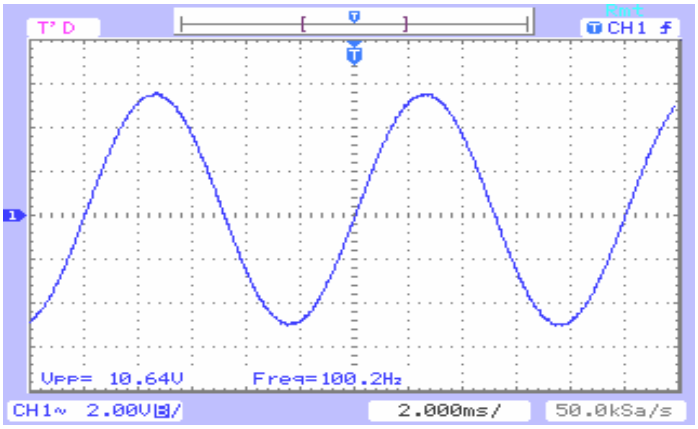

Figure 5-3: Input signal without any noise and differentiated output obtained

`

The output of the amplitude modulation using the multiplier AD633 is shown in Figure 5.4. The magnitude of the amplitude modulated signal can be increased by increasing the magnitude of the modulating signal using a variable gain amplifier. The modulation index of the modulated signal is 100% as DSBSC is implemented.

The frequency response of the differentiator used is shown in Figure 5.5. The zero of the circuit is located at 15 Hz and two intersecting poles are located at 15.6 KHz. The gain of the circuit has a slope of +20dB and crosses 0dB at the frequency where the zero is located. The slope is -20dB after the pole frequency. The time response of the carrier wave after differentiation is shown in Figure 5.6. The output is 90 degree phase shifted with respect to the carrier wave. The differentiation of amplitude modulated signal is also calculated.

The amplitude modulated differentiator and the carrier differentiated amplitude modulated signal are given as inputs to the summing amplifier. Figure 5.7 shows the output from the summing amplifier.

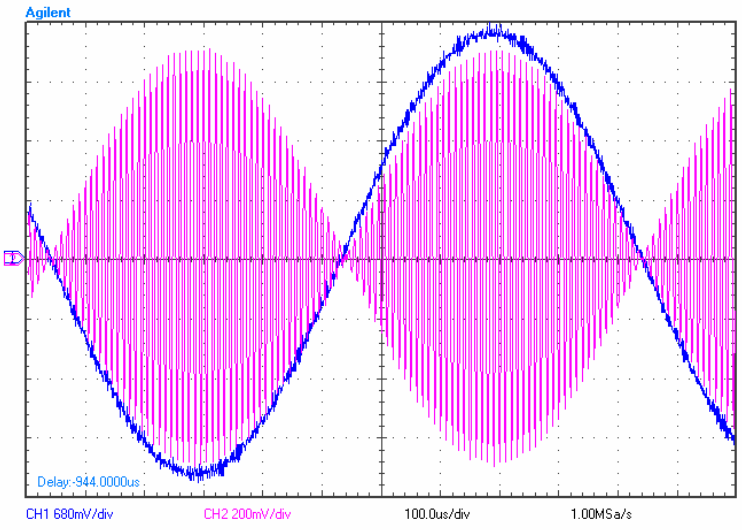

Figure 5-4: Amplitude modulation

`

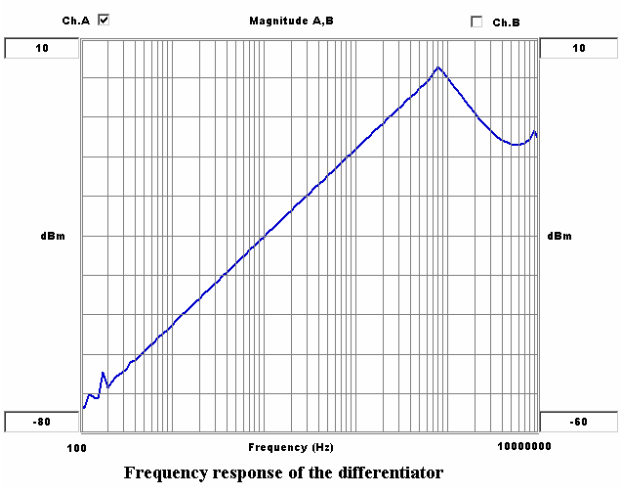

Figure 5-5: Frequency response of the differentiator measured in Sleuth

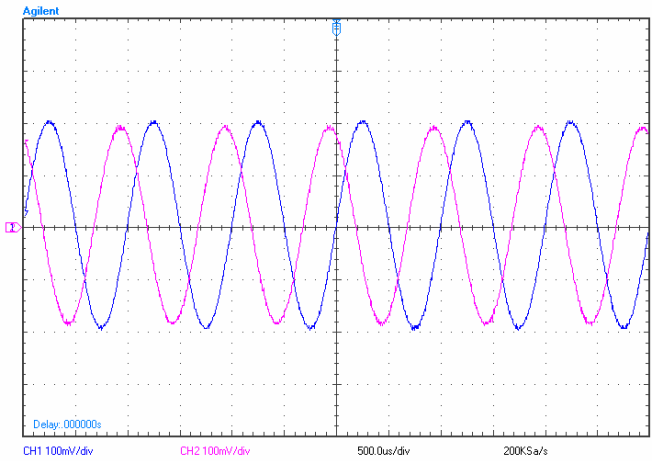

Figure 5-6: Differentiator output

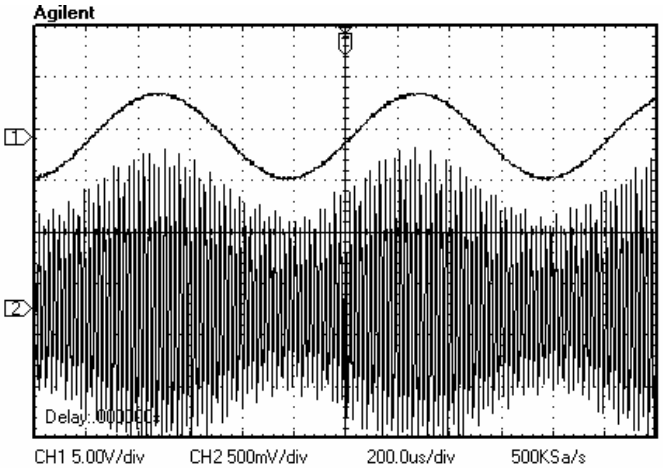

Figure 5-7: Output from the summer

`

The output form the summer is given to the demodulator. The output from the demodulator is shown in Figure 5.8. This signal is amplified and given to the low pass filter circuit. The output of the filter which is the final output of the entire circuit is shown in Figure 5.9.

The output of the differentiator is verified by giving a triangular wave input. The obtained square wave is shown in Figure 5.10. The SNR of the output can be increased using higher carrier frequencies.

The limitation of using a higher frequency carrier signal is that the magnitude of the output during differentiation exceeds the rail to rail voltage of the op amp. If the carrier is increased further clipping will occur making the output signal irretrievable. The phase difference between the input and the output also changes when using higher frequency due to the effect of two intercepting poles. The maximum carrier frequency used during simulation is 30 KHz.

The temperature data as shown in Figure 5.11(a) is given as the input signal to the sensor interface. The expected differentiated output is shown in the Figure 5.11(b). The amplitude modulated wave is shown in Figure 5.12 and the output differentiated signal is shown in Figure 5.13.

The output differentiated signal is acquired into computer using the scope probe software for measuring the signal-to-noise ratio. The sampling rate can also be changed by using Labview interface. Signal-to-noise in the experiments also improves with increase in carrier frequencies but they are not equal to the SNR's obtained during simulations. The SNR obtained during experiments is shown in Figure 5.14. The curve is linear and it increases with increase in carrier frequency.

`

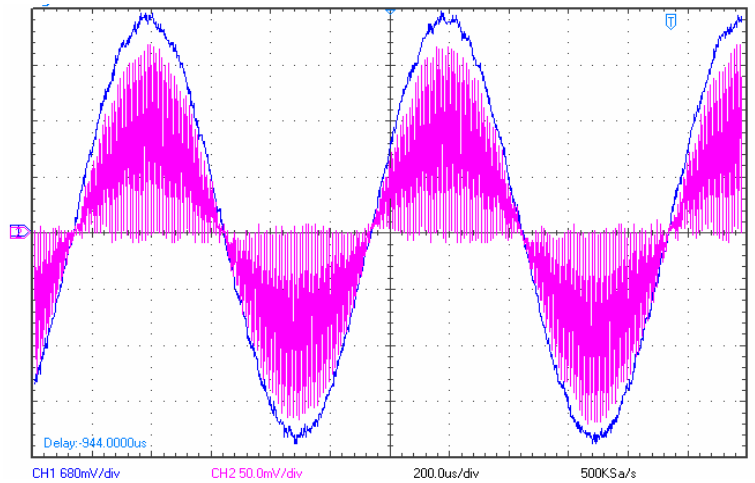

Figure 5-8: Demodulated output

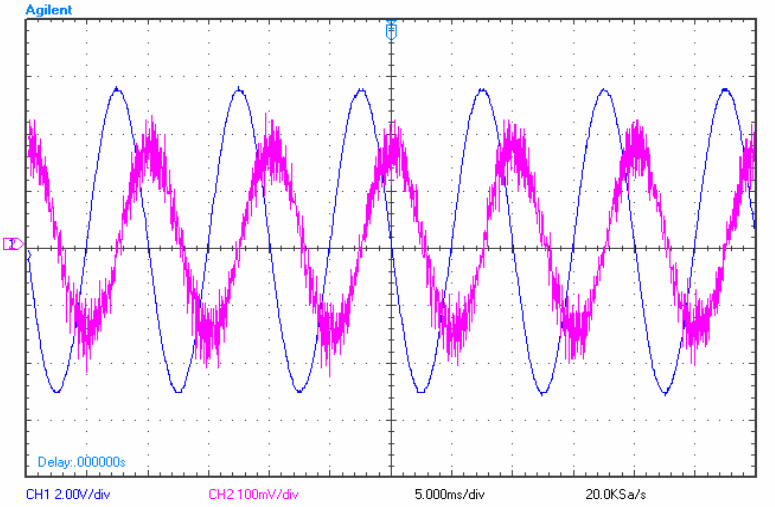

Figure 5-9: Filtered output

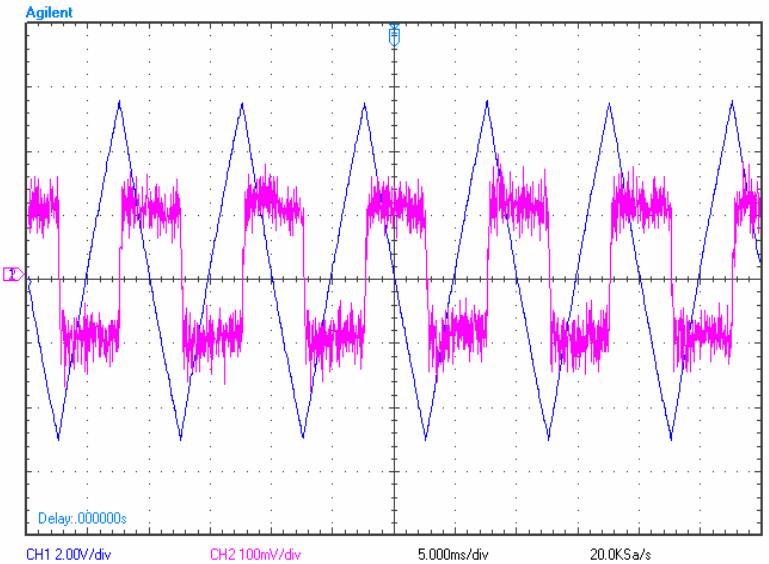

Figure 5-10: Square wave output using a triangular input

`

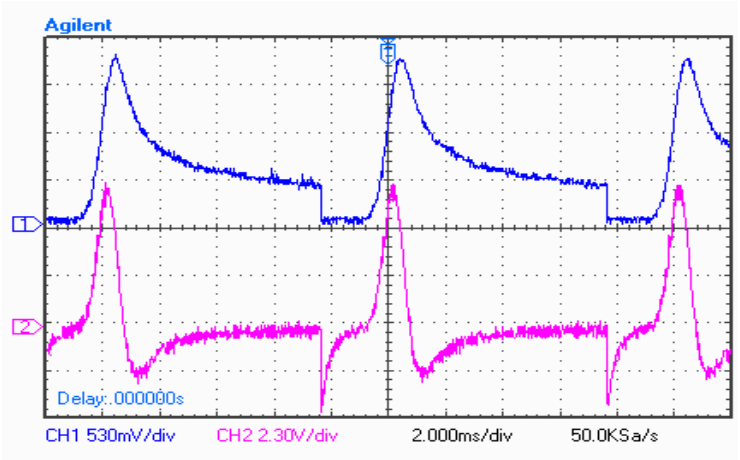

Figure 5-11: Temperature data and desired output data

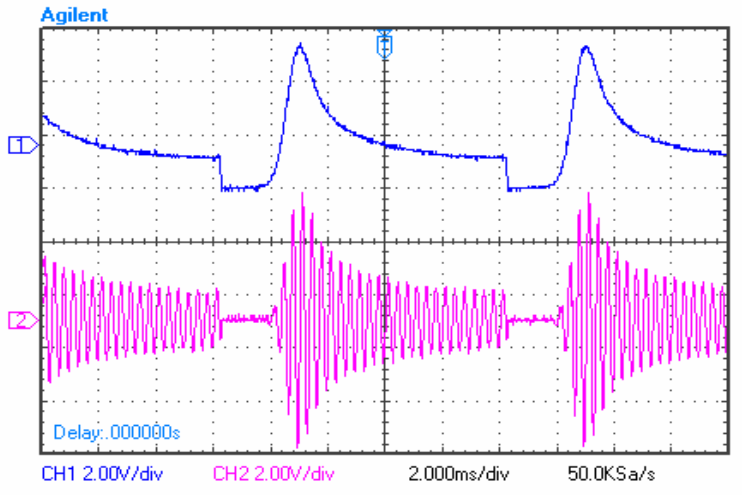

Figure 5-12: Amplitude modulation of temperature data

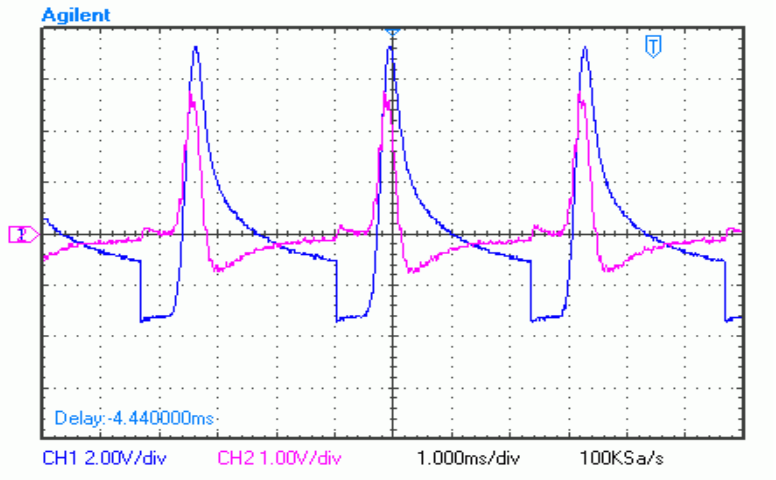

Figure 5-13: Output differentiated waveform obtained

`

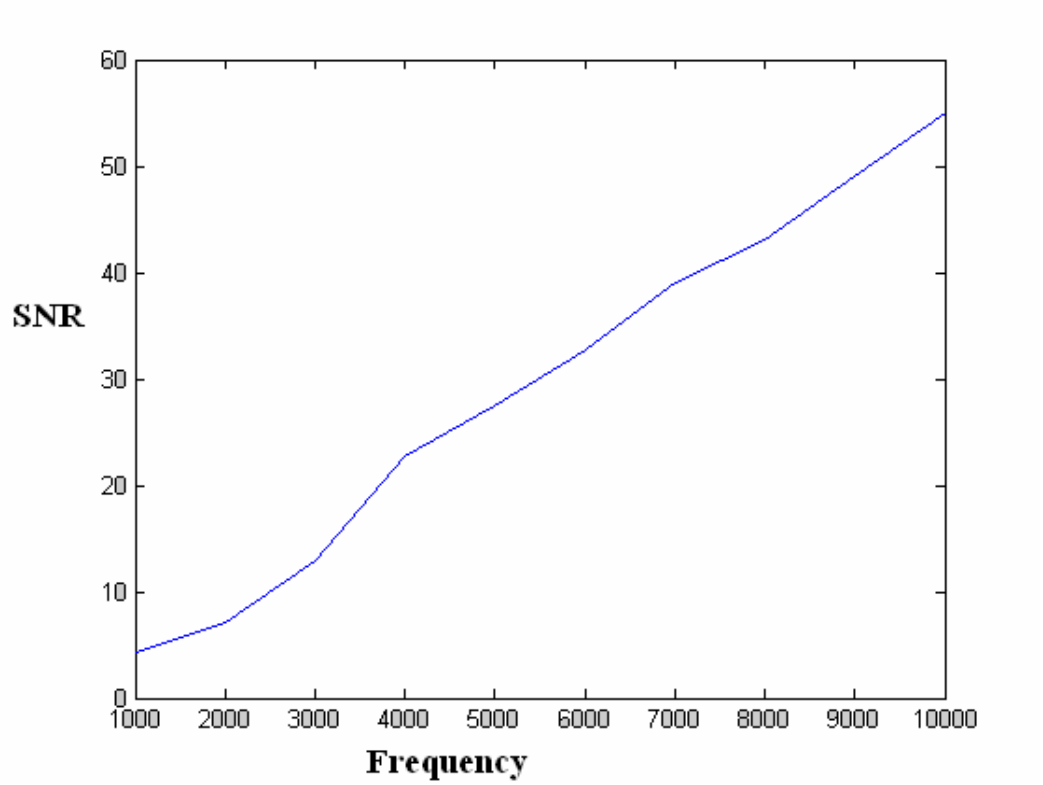

Figure 5-14: SNR obtained during experiment using different carrier frequencies

5.3 Problems Encountered

The improvements in signal-to-noise ratio are comparatively lesser in magnitude during the experimental due to external noise added by long wires and power supply connections.

This external noise can be significantly reduced by having a prototype PCB board designed for this purpose. However, the design would be based on a single carrier frequency and subsequent increments in the carrier frequency would necessitate for a different board design. The PCB board design also dependents on the modulating frequency. Hence it would be impractical to design a PCB board.

The limitations of op amp limit the usage of higher carrier frequency in the experiment. The gain during differentiation of the carrier frequency increases beyond the rail-to-rail voltage of the op amp. On reducing the gain of the differentiator, the

magnitude of the output voltage obtained is low and cannot be retrieved after demodulation.

Also, there should be an exact 180 degree phase difference between the undesired signals viz. the differentiated amplitude modulated signal and the signal obtained from amplitude modulation of the differentiated carrier. This would ensure cancellation of the two undesired signals. The signal-to-noise ratio deteriorates if the phase difference is not maintained. Precautions are taken to avoid these detrimental factors.

The signal to noise ratio increases with increase in carrier frequency. The final conclusions of the present work are explained in Chapter 6.

CHAPTER 6: CONCLUSIONS

The goal to improve the signal-to-noise ratio has been achieved by using universal voltage rate sensor interface. It was first proved mathematically using equations and later using Matlab simulations. The experiments were done based on PSpice simulation results. The signal-to-noise ratio improved in both cases. However, improvement in signal-to-noise ratio during experiments was equal to that in simulations due to external noise factors and opamp limitations.

It can be incurred that SNR of temperature data when differentiated at low frequency is low. The signal-to-noise ratio improves when the noisy signal is passed through a filter before differentiation by removing high frequency noise. The signal-to-noise ratio is further increased if the signal is amplitude modulated and differentiated at higher frequency which also validates the theoretical proposal of the project.

The predicted heat flux using heating/cooling rate data obtained using universal voltage rate sensor interface is reliable and will not have any ill-posed effects.

REFERENCES

[1] Frankel J.I., "Regularization of inverse heat conduction by combination of rate sensor and analytic continuation," 2007, J Eng Math Vol. 57 pp 181-198.

[2] Frankel J.I., and Arimilli R.V., "Inferring convective and radiative heating loads from transient surface temperature measurement in the half space," 2007, Inverse problems in science and engineering, Vol. 15, No. 5, pp. 463-488

[3] Frankel J.I., Arimilli R.V., Keyhani M., and Wu J., Heating Rate dT/dt Measurements Developed from In-Situ Thermocouples using a Voltage-Rate Interface for Advanced Thermal Diagnostics

[4] Frankel J.I., and Wu J., "Universal voltage-rate sensor interface for real-time evaluation of rate-based quantities" 2006, (in press).

[5] Frankel J. I., "Thermal-Rate Based Sensor Development for Stabilizing Ill-Posed Problems and for Use in Real-Time Diagnostics", 55th International Astronautically Congress, Vancouver, Canada, October 4-8, 2004.

[6] http://www.sysf.physto.se/kurser/matteknik/lab4/ModulationLab.pdf (AM)

[7] http://www.mathworks.com/access/helpdesk/help/techdoc/matlab.shtml

[8] http://www.seas.upenn.edu/~jan/spice/spice.overview.html

[9] http://www.jaycar.com.au/images_uploaded/XR2206V1.PDF

[10] http://focus.ti.com/lit/an/sloa024b/sloa024b.pdf

`

[11] http://www.engr.siu.edu/staff2/spezia/Web438A/labs/LAB38A4.pdf

[12] http://www.analog.com/UploadedFiles/Data_Sheets/AD633.pdf

[13] http://www.electronics.dit.ie/staff/ypanarin/Lecture%20Notes/DT021-4/7AnalogMultipliers.pdf

[14] http://web.mit.edu/6.301/www/OP27c.pdf

[15] http://www.analogzone.com/col_01302004.pdf

[16] www.national.com/an/AN/AN-31.pdf

[17] http://cp.literature.agilent.com/litweb/pdf/5988-8544EN.pdf

[18] http://cp.literature.agilent.com/litweb/pdf/5989-2235EN.pdf

[19] http://www.ni.com/swf/presentation/us/labview/aap/default.htm

[20] http://www.accusystemscorp.com/AccuCore/CoreTechnologyDataSheet.htm

APPENDIX

A.1 Matlab code for finding SNR

```
close all;
clear all;
% Generating Modulating signal
r=3
[t,y] = textread('d1.csv','%n%n%*[^\n]','headerlines',0,'delimiter',',');
b=length(y);
t=0.01/b:0.01/b:0.01;
for i=1:2
   t=av(t);
   y=av(y);
end

[t1,xm] = textread('d2.csv','%n%n%*[^\n]','headerlines',0,'delimiter',',');
for i=1:2
   xm=av(xm);
end
fid=fopen('t.txt','wt');
dataset=[t;y];
fprintf(fid,'%6.10f,%12.10f,',dataset);
st=t(length(t));
L=length(xm);
Fs=L/st;
NFFT =2^nextpow2(2^23);
wn=1000/Fs;
[b,a]=butter(1,wn);
fxm=filter(b,a,xm);
fy=filter(b,a,y);
wn=1000/Fs;
[b,a]=butter(1,wn);
ffy=filter(b,a,fy);
%differetiate the carrier signal with out noise
dt=t(2)-t(1);
for i=2:length(xm)
py(i)=1e-3*(y(i)-y(i-1))/dt;
end
%differetiate the carrier signal with out noise
for i=2:length(xm)
pfy(i)=1e-3*(fy(i)-fy(i-1))/dt;
end
%differetiate the carrier signal with out noise
for i=2:length(xm)
pffy(i)=1e-3*(ffy(i)-ffy(i-1))/dt;
end
fid = fopen('data.txt', 'w');
fwrite(fid,y)
%differetiate the input signal with noise
dt=t(2)-t(1);
for i=2:length(xm)
pxm(i)=1e-3*(xm(i)-xm(i-1))/dt;
end
%differetiate the filtered signal
for i=2:length(xm)
`
```

```
pfxm(i)=1e-3*(fxm(i)-fxm(i-1))/dt;
end

pfy=pfy*max(py)/max(pfy);
pxm=pxm*max(py)/max(pxm);
pfxm=pfxm*max(py)/max(pfxm);
snr_py=0;
snr_pfy=0;
snr_pxm=0;
snr_pfxm=0;
for i=1:length(xm)
   snr_py=snr_py+py(i)^2;
   snr_pfy=snr_pfy+pfy(i)^2;
   snr_pxm=snr_pxm+pxm(i)^2;
   snr_pfxm=snr_pfxm+pfxm(i)^2;
end
snr_dxm=(snr_py/(snr_pxm-snr_py))
snr_f_dxm=(snr_pfy/(snr_pfxm-snr_pfy))
% Carrier Signal
fc=input('enter the carrier frequency');
xc=sin(2*pi*t*fc);


%differetiate the carrier signal

for i=2:length(xc)
pxc(i)=1e-3*(xc(i)-xc(i-1))/dt;
end

%Amplitude modulation
for i=1:length(t)
      xm1(i)=xm(i)*xc(i); % am wave with noise
      xm2(i)=xm(i)*pxc(i);
      xm0(i)=fxm(i)*xc(i);%am wave without noise
      xm3(i)=fxm(i)*pxc(i);
end

%Differentiation of am signal
dt=t(2)-t(1);
for i=2:length(xm1)
dxm1(i)=-1e-3*(xm1(i)-xm1(i-1))/dt;% with noise
dxm0(i)=-1e-3*(xm0(i)-xm0(i-1))/dt;% without noise
end

%adder
for i=1:length(xm1)
   ad(i)=dxm1(i)+xm2(i);%noise
   ad1(i)=dxm0(i)+xm3(i);%without noise
end

%product multiplier
   for i=1:length(t)
      dx(i)=ad(i)*xc(i);       %noise
      dx1(i)=ad1(i)*xc(i);     %without noise
   end
`
```

```
 % Low pass filter
    wn=1000/Fs;
    [b,a]=butter(1,wn);
    %b =[0.0887e-4,0.1774e-4,0.0887e-4];
    %a =[1.0000   -1.9916    0.9916];
    out=-filter(b,a,dx);%noise
    out1=-filter(b,a,dx1);%without noise
    fy2=filter(b,a,y);
for i=2:length(xm1)
pfy2(i)=1e-3*(fy2(i)-fy2(i-1))/dt;% with noise
end

    pffy=pffy*max(pfy2)/max(pffy);
    out=out*max(pfy2)/max(out);
    out1=out1*max(pfy2)/max(out1);

snr_pfy2=0;
snr_pffy=0;
snr_out=0;
snr_out1=0;
for i=1:length(xm)
    snr_pfy2=snr_pfy2+pfy2(i)^2;
    snr_pffy=snr_pffy+pffy(i)^2;
    snr_out=snr_out+out(i)^2;
    snr_out1=snr_out1+out1(i)^2;
end
snr_noise=(snr_pfy2/(snr_out-snr_pfy2))
snr_filtered=(snr_pffy/(snr_out1-snr_pffy))

%figure 2
figure;
subplot(4,2,1);
plot(t,xm);
subplot(4,2,2);
plot(t,xc);
subplot(4,2,3);
plot(t,xm1);
subplot(4,2,4);
plot(t,xm2);
subplot(4,2,5);
plot(t,dxm1);
subplot(4,2,6);
plot(t,ad);
subplot(4,2,7);
plot(t,dx);
subplot(4,2,8);
plot(t,out);



% %figure
% FFT of mod
  Y1 = fft(y,NFFT)/L;
  f = Fs/2*linspace(0,1,NFFT/2);
`
```

```
%FFT of the carrier signal
Y2 = fft(py,NFFT)/L;
figure;
subplot(1,2,1)
plot(t,y,t,py);
xlabel('time');
ylabel('magnitude');
subplot(1,2,2);
plot(f(1:10000),2*abs(Y1(1:10000)),f(1:10000),2*abs(Y2(1:10000)))
xlabel('Frequency');
ylabel('dB');
%
% %FFT of the am signal
 Y = fft(xm1,NFFT)/L;
 subplot(4,2,3);
 plot(f(1:100000),2*abs(Y(1:100000)))
 title('FFT of the phase shifted am signal');
 xlabel('Frequency');
 ylabel('dB');

% %FFT of the differentiated carrier am signal
 Y = fft(xm2,NFFT)/L;
 subplot(4,2,4);
 plot(f(1:100000),2*abs(Y(1:100000)))
 title('FFT of the phase shifted am signal');
 xlabel('Frequency');
 ylabel('dB');

%  %FFT of the diffrentiated am signal
 Y = fft(dxm1,NFFT)/L;
 subplot(4,2,5);
 plot(f(1:100000),2*abs(Y(1:100000)))
 title('FFT of the phase shifted am signal');
 xlabel('Frequency');
 ylabel('dB');

%  %FFT of the adder
 Y = fft(xm2,NFFT)/L;
 subplot(4,2,6);
 plot(f(1:100000),2*abs(Y(1:100000)))
 title('FFT of the phase shifted am signal');
 xlabel('Frequency');
 ylabel('dB');

%  %FFT of the demodulated am signal
 Y = fft(xc,NFFT)/L;
 subplot(4,2,7);
 plot(f(1:100000),2*abs(Y(1:100000)))
 title('FFT of the phase shifted am signal');
 xlabel('Frequency');
 ylabel('dB');
```

`

```
 %FFT of the output signal
 Y = fft(xc,NFFT)/L;
 subplot(4,2,8);
 plot(f(1:100000),2*abs(Y(1:100000)))
 title('FFT of the phase shifted am signal');
 xlabel('Frequency');
 ylabel('dB');

figure;
subplot(2,2,1);
plot(t,py,t,pxm);
subplot(2,2,2);
plot(t,pfy,t,pfxm);
subplot(2,2,3);
plot(t,pfy2,t,out);
subplot(2,2,4);
plot(t,pffy,t,out1);

figure;
plot(t,y,t,py);
```

A.2 PSPICE output file

**** 11/04/07 16:54:16 ******* PSpice 15.7.0 (July 2006) ****** ID# 30407096 *

 * Multiplier

 ****   CIRCUIT DESCRIPTION

****

.inc 'ad633.txt'

**** INCLUDING ad633.txt ****
* AD633 Analog Multiplier Macro Model 12/93, Rev. A
* AAG/PMI
*
* Copyright 1993 by Analog Devices, Inc.
*
* Refer to "README.DOC" file for License Statement. Use of this model
* indicates your acceptance with the terms and provisions in the License Statement.
*
* Node assignments
*   X1
* | X2
* | | Y1
* | | | Y2
* | | | | VNEG
* | | | | | Z
* | | | | | | W
* | | | | | | | VPOS
* | | | | | | | |
.SUBCKT AD633 1 2 3 4 5 6 7 8
*
EREF 100 0 POLY(2) 8 0 5 0 (0,0.5,0.5)
*
* X-INPUT STAGE & POLE AT 15 MHz
*
IBX1 1 0 DC 8E-7
IBX2 2 0 DC 8E-7
EOSX 10 1 POLY(1) (16,100) (5E-3,1)
RX1A 10 11 5E6
RX1B 11 2 5E6
*
GX 100 12 10 2 1E-6
RX 12 100 1E6
CX 12 100 1.061E-14
VX1 8 13 DC 3.05
DX1 12 13 DX
VX2 14 5 DC 3.05

`

```
DX2 14 12 DX
*
* COMMON-MODE GAIN NETWORK WITH ZERO AT 560 Hz
*
ECMX 15 100 11 100 10
RCMX1 15 16 1E6
CCMX 15 16 2.8421E-10
RCMX2 16 100 1
*
* Y-INPUT STAGE & POLE AT 15 MHz
*
IBY1 3 0 DC 8E-7
IBY2 4 0 DC 8E-7
EOSY 20 3 POLY(1) (26,100) (5E-3,1)
RY1A 20 21 5E6
RY1B 21 4 5E6
*
GY 100 22 20 4 1E-6
RY 22 100 1E6
CY 22 100 1.061E-14
VY1 8 23 DC 3.05
DY1 22 23 DX
VY2 24 5 DC 3.05
DY2 24 22 DX
*
* COMMON-MODE GAIN NETWORK WITH ZERO AT 560 Hz
*
ECMY 25 100 21 100 10
RCMY1 25 26 1E6
CCMY 25 26 2.8421E-10
RCMY2 26 100 1
*
* Z-INPUT STAGE & POLE AT 15 MHz
*
IBZ1 7 0 DC 8E-7
IBZ2 6 0 DC 8E-7
RZ1 7 6 10E6
*
GZ 100 32 7 6 1E-6
RZ2 32 100 1E6
CZ 32 100 1.061E-14
VZ1 8 33 DC 3.05
DZ1 32 33 DX
VZ2 34 5 DC 3.05
DZ2 34 33 DX
*
* 50-MHz MULTIPLIER CORE & SUMMER
*
GXY 100 40 POLY(2) (12,100) (22,100) (0,0,0,0,0.1E-6)
RXY 40 100 1E6
CXY 40 100 3.1831E-15
*
* OP AMP INPUT STAGE
*
VOOS 59 40 DC 5E-3
`
```

```
Q1 55 32 60 QX
Q2 56 59 61 QX
R1 8 55 3.1831E4
R2 60 54 3.1313E4
R3 8 56 3.1831E4
R4 61 54 3.1313E4
I1 54 5 1E-4
*
* GAIN STAGE & DOMINANT POLE AT 316.23 Hz
*
G1 100 62 55 56 3.141637E-5
R5 62 100 1.0066E8
C3 62 100 5E-12
V1 8 63 DC 4.3399
D1 62 63 DX
V2 64 5 DC 4.3399
D2 64 62 DX
*
* NEGATIVE ZERO AT 20 MHz
*
ENZ 65 100 62 100 1E6
RNZ1 65 66 1
FNZ 65 66 VNC -1
RNZ2 66 100 1E-6
ENC 67 0 65 66 1
CNZ 67 68 7.9577E-9
VNC 68 0 DC 0
*
* POLE AT 4 MHz
*
G2 100 69 66 100 1E-6
R6 69 100 1E6
C2 69 100 3.9789E-14
*
* OP AMP OUTPUT STAGE
*
FSY 8 5 POLY(2) VZC1 VZC2 (2.8286E-3,1,1)
RDC 8 5 28E3
GZC 100 73 72 69 11.623E-3
VZC1 74 100 DC 0
DZC1 73 74 DX
VZC2 100 75 DC 0
DZC2 75 73 DX
VSC1 70 72 0.695
DSC1 69 70 DX
VSC2 72 71 0.695
DSC2 71 69 DX
GO1 72 8 8 69 11.623E-3
RO1 8 72 86
GO2 5 72 69 5 11.623E-3
RO2 72 5 86
LO 72 7 1E-7
*
* MODELS USED
*
`
```

```
.MODEL QX NPN(BF=1E4)
.MODEL DX D(IS=1E-15)
.ENDS AD633

**** RESUMING total.cir ****
.inc 'op27.txt'

**** INCLUDING op27.txt ****
.SUBCKT OP-27    2     3    4     6    7
*              -IN   +IN   VEE   OUT   VCC
* DEVICE CHAR:  AOL=1.5E6, ZIN=4MEG// 8PF, IB= 15NA,IOS=12NA,RCM=2E9
*               RO=70, GB=8MHZ,SR=2.8V/US, VOS=30UV, CMRR=120DB,PSRR=2UV/V
*               VINCM=+-12.5V, VO=+-13.5V, IO(LIMIT)= +35MA,-42MA; POLES AT
*               5.3HZ;0.8,12,20,30 MHZ; ZEROES AT 0.9,6.5 MHZ. EN=3NV/RTHZ
*               IN=0.4PA/RTHZ, FB(IN)=140 HZ.LAST NODE=31
*
VOS 2 23 30U
ECMRR 23 24 POLY(2) 22 0 3 0 0 0.5U 0.5U
EPSRR 24 22 POLY(2) 7 0 4 0 60U -2U 2U
IOSI 0 2 479NA
RCMI 2 0 4000MEG
CIN 2 3 8PF
RCMN 3 0 4000MEG
IOSN 0 3 491NA
VP 11 0 42.6
R1 11 5 3.36K
R2 11 10 3.36K
CC 5 25 25.94PF
RZ1 25 10 943.2
Q1 5 22 1 N1
Q2 10 3 9 N1
RE1 1 8 109
RE2 8 9 109
ICS 8 14 17.94MA
VN 0 14 15
D1 12 8 DA
R3 12 13 100
V1 13 14 1.4
G1 0 15 5 10 10M
R4 15 0 5MEG
D2 15 17 DB
D3 17 15 DB
E1 17 0 16 0 1
R5 15 16 50
C1 16 0 5.963NF
E3 26 0 16 0 1
RA1 26 27 1.325K
CA1 27 0 10PF
E4 28 0 27 0 1
RA2 28 29 795
CA2 29 0 10PF
E5 30 0 29 0 33.33
RA3 30 31 3.233K
CA3 30 31 54.64PF
RA4 31 0 100
`
```

```
G2 0 18 31 0 0.02
R6 18 0 50
D4 18 19 DA
D5 19 18 DC
E2 19 0 6 0 1
R7 18 6 20
D6 6 20 DA
D7 21 6 DA
V3 7 20 2.2
RPS 7 4 26K
IPS 7 4 1.9MA
V2 21 4 2.2
.MODEL DA D(IS=5.73E-14)
.MODEL DB D(IS=1.47E-16)
.MODEL DC D(IS=3.07E-16)
.MODEL N1 NPN(IS=1FA BF=1.79E4 RB=150 KF=4.5E-17)
*
.ENDS OP-27



**** RESUMING total.cir ****
VCC 98 0 15
VEE 99 0 -15


V1 1 0 sin(0 0.1 13000)
V2 26 0 pwl(0 0 2.5m 5 5m 0 7.5m -5 10m 0 12.5m 5 15m 0 17.5m -5 20m 0)
V3 25 0 pwl(0 0 2.5m 1 5m 0 7.5m -1 10m 0 12.5m 1 15m 0 17.5m -1 20m 0)
*V4 31 0 sin(0 0.01 500)

*Summing amplifier
R17 26 24 1k
R18 25 24 1k
*R23 31 24 2k
R19 23 0 1k
R20 23 2 1k

*Multipliers
X2 1 0 2 0 99 0 3 98 AD633


*Differentiator
X4 5 0 99 6 98 OP-27
*R1 3 4 10
C1 3 5 1u
R2 5 6 1k
*C2 5 6 1n


*Differentiator
X5 9 0 99 10 98 OP-27
*R3 1 8 10
C3 1 9 1u
R4 9 10 1k
`
```

```
*C4 9 10 1n

* Inverter
X6 7 0 99 12 98 OP-27
R5 10 7 1k
R6 7 12 1k


*Multiplier
X3 2 0 12 0 99 0 11 98 AD633


*inverting amp to remove offset
X24 100 0 99 97 98 OP-27
X25 101 82 99 96 98 OP-27

R100 6 100 1k
R97 100 97 2k

R101 11 101 1k
R96 101 96 2k
R82 82 0 500


*Summing Amplifier
X8 14 13 99 15 98 OP-27

R7 96 13 1k
R8 97 13 1k
R9 14 0 1k
R10 14 15 1k


*Multiplier
X7 15 0 48 0 99 45 16 98 AD633
R45 16 45 1k
R46 45 0 3k

*Low pass filter
X9 19 18 99 20 98 OP-27
R11 16 17 1.59k
R12 17 18 1.59k
C5 18 0 .1u
C6 17 20 .1u
R13 19 0 10k
R14 19 20 5.6k

*Amplifier
X10 21 40 99 22 98 OP-27
R15 40 0 1k
R16 21 22 10k
R30 20 21  1k

*Amplifier
X14 47 1 99 48 98 OP-27
`
```

```
R47 47 0 1k
R48 47 48 10k


*Summing Amplifier
X11 23 24 99 2 98 OP-27

*differentiator of noise signal at low frequency
X12 28 0 99 29 98 OP-27
*R22 2 27 100
C7 2 28 .1u
R21 28 29 1k
*C8 28 29 10n

*differentiator of original signal at low frequency
X13 33 0 99 34 98 OP-27
*R32 26 32 100
C9 26 33 .1u
R33 33 34 1k
*C10 33 34 10n


.TRAN 0.1u 20m
.OP
.PROBE
.END

**** 11/04/07 16:54:16 ******* PSpice 15.7.0 (July 2006) ****** ID# 30407096 *

 NODE   VOLTAGE    NODE   VOLTAGE    NODE   VOLTAGE    NODE   VOLTAGE


( 1)       0.0000     ( 2)      72.00E-06     ( 3)       .0050     ( 5)      30.00E-06
(  6)      52.08E-06   (7)      30.00E-06     ( 9)       30.00E-06 (10)      52.08E-06
(11)       .0050      ( 12)     30.00E-06     (13)       -.0049    ( 14)     -.0049
(15)       -.0098     (16)      .0175         (7)        .0175     (18)      .0175
(19)       .0175      (20)      .0275         (21)       20.11E-06 (22)      -.2741
(23)       24.96E-06  (24)      -5.038E-06    (25)       0.0000    (26)      0.0000
(28)       30.00E-06  (29)      52.08E-06     (33)       30.00E-06 (34)      52.08E-06
(40)       -10.08E-06 (45)      .0125         (47)       30.00E-06 (48)      550.8E-06
(82)       -5.038E-06 (96)      -.0099        (97)       30.00E-06 (98)      15.0000
(99)       -15.0000   (100)     30.00E-06     (101)      24.97E-06


 * Multiplier
 ****     JOB STATISTICS SUMMARY
******************************************************************************
  Total job time (using Solver 1)   =       50.14
```

`

VITA

Jayanth Chakradhar Kruttiventi was born in Hyderabad, AP, India on July 8 1982. He attained his bachelor's degree in electronics and communications engineering from Mahatma Gandhi Institute of Technology an affiliated institute to Jawaharlal Nehru Technological University. After graduating with flying colors, he gained additional expertise in IT by learning wide range of software languages. To gain expertise in the field of analog VLSI he joined prestigious University of Tennessee, Knoxville. He completed his Masters under the guidance of Dr. Jie Wu in year 2007.